CENTRAL RESEARCH LIBRARY
DOCUMENT COLLECTION

[redacted]

[redacted]

MARTIN MARIETTA ENERGY SYSTEMS LIBRARIES
3 4456 0360606 0

INV 65

ORNL 1371
Radiation Effects on Reactor Materials

4A

LABORATORY RECORDS
1954

GAMMA RADIATION INDUCED IN ENGINEERING MATERIALS

C. D. Bopp

CENTRAL RESEARCH LIBRARY
DOCUMENT COLLECTION

LIBRARY LOAN COPY

DO NOT TRANSFER TO ANOTHER PERSON

If you wish someone else to see this document, send in name with document and the library will arrange a loan.

OAK RIDGE NATIONAL LABORATORY
OPERATED BY
CARBIDE AND CARBON CHEMICALS COMPANY
A DIVISION OF UNION CARBIDE AND CARBON CORPORATION
UCC
POST OFFICE BOX P
OAK RIDGE, TENNESSEE

[redacted]

[redacted]

[redacted]

ORNL 1371

This document consists of 63 pages.
Copy 4 of 164 copies. Series A.

Contract No. W-7405-eng-26

SOLID STATE DIVISION

ENGINEERING PROPERTIES SECTION

GAMMA RADIATION INDUCED IN ENGINEERING MATERIALS

C. D. Bopp

Measurements by: W. K. Kirkland and R. L. Towns

DECLASSIFIED

CLASSIFICATION CHANGED TO:

BY AUTHORITY OF: TID-1148

BY: R. Morrison 7/22/57

DATE ISSUED

APR 16 1953

OAK RIDGE NATIONAL LABORATORY
Operated by
CARBIDE AND CARBON CHEMICALS COMPANY
A Division of Union Carbide and Carbon Corporation
Post Office Box P
Oak Ridge, Tennessee

MARTIN MARIETTA ENERGY SYSTEMS LIBRARIES

3 4456 0360606 0

[redacted]

INTERNAL DISTRIBUTION

1. C. E. Center
2. Biology Library
3. Health Physics Library
4-5. Central Research Library
6. Reactor Experimental Engineering Library
7-12. Central Files
13. C. E. Larson
14. W. B. Lewis (K-25)
15. L. B. Emlet (Y-12)
16. A. M. Weinberg
17. E. H. Taylor
18. E. D. Shipley
19. D. S. Billington
20. F. C. VonderLage
21. R. C. Briant
22. J. A. Swartout
23. S. C. Lind
24. F. L. Steahly
25. A. H. Snell
26. A. Hollaender
27. M. T. Kelley
28. G. H. Clewett
29. K. Z. Morgan
30. J. S. Felton
31. A. S. Householder
32. C. S. Harrill
33. C. E. Winters
34. D. W. Cardwell
35. E. M. King
36. A. J. Miller
37. J. T. Howe
38. D. D. Cowen
39. H. F. Poppendiek
40. A. R. Olsen
41. R. N. Lyon
42. W. K. Ergen
43. E. P. Blizard
44. J. A. Cox
45. C. D. Cagle
46. F. M. Tench, Jr.
47. T. H. Blewitt
48. J. H. Crawford
49. J. B. Trice
50. O. Sisman
51. W. L. Ross
52. H. L. F. Enlund
53. C. G. Heisig
54. W. W. Parkinson
55. C. D. Baumann
56. W. E. Brundage
57. C. D. Bopp
58. W. K. Kirkland
59. R. L. Towns
60. S. E. Dismuke
61. G. W. Keilholtz
62. R. H. Kernohan
63. J. B. Trice
64. J. C. Wilson
65. M. E. Ramsey
66. G. C. Williams
67. [illegible] M. Reyling
68. [illegible] B. Briggs

EXTERNAL DISTRIBUTION

69-76. Argonne National Laboratory
77. Armed Forces Special Weapons Project, Washington
78. Army Chemical Center
79-82. Atomic Energy Commission, Washington
83. Battelle Memorial Institute
84-86. Brookhaven National Laboratory
87. Bureau of Ships
88-89. California Research and Development Company
90-95. Carbide and Carbon Chemicals Company (Y-12 Plant)
96. Chicago Patent Group

[redacted]

[redacted]

This [redacted] the [redacted] manner to an unauthorized person is prohibited.

[redacted]

97-101. duPont Company
102-104. General Electric Company (ANPP)
105-108. General Electric Company, Richland
109. Hanford Operations Office
110-113. Idaho Operations Office
114. Iowa State College
115-118. Knolls Atomic Power Laboratory
119-120. Los Alamos Scientific Laboratory
121. Massachusetts Institute of Technology (Kaufmann)
122. National Advisory Committee for Aeronautics, Cleveland
123-124. New York Operations Office
125-127. North American Aviation, Inc.
128. Nuclear Development Associates, Inc.
129. Patent Branch, Washington
130. Rand Corporation
131. Savannah River Operations Office, Augusta
132. Savannah River Operations Office, Wilmington
133. Sylvania Electric Products, Inc.
134-135. University of California Radiation Laboratory
136. Vitro Corporation of America
137. Walter Kidde Nuclear Laboratories, Inc.
138-141. Westinghouse Electric Corporation
142-149. Wright Air Development Center
150-164. Technical Information Service, Oak Ridge

[redacted]

[redacted]

ABSTRACT

The gamma activity induced in engineering materials in the X-reactor was measured for long pile exposures, and long decay periods. The decay curves were resolved into component activities which were tabulated so that the activity for any irradiation period and any decay period may be calculated. The half thicknesses of lead were determined from absorption measurements.

TABLE OF CONTENTS

	Page No.
ABSTRACT	3
INTRODUCTION	6
Index to Decay Curves	8
RESULTS	10
Analysis of Decay Curves	10
Saturated Values of Component Activities of Decay Curves	13
Calculation of Activity	16
Absorption Measurements	17
Half Thickness of Lead	23
DISCUSSION	26
EXPERIMENTAL	30
BIBLIOGRAPHY	31
ACKNOWLEDGMENTS	31
APPENDIX I	32
Calculation of rep/hr	32
APPENDIX II	33
Decay Curves	33

LIST OF TABLES & FIGURES

		Page No.
Table I	Nominal Composition of the Materials and Index to the Decay Curves	8
Table II	Saturated Values of the Component Activities	13
Table III	Product of the Isotopic Cross Section and the Number of Target Atoms per Gram of Element, N	18
Table IV	Ion Chamber Response for the Isotopes	19
Table V	Calculated Values of Induced Activity Compared with Measured Values for the Isotopes	20
Table VI	Absorption of Gamma Radiation from the Materials	23
Figure 1	Analysis of Decay Curve for 347 Stainless Steel	12
Figure 2	Absorption of Gamma Radiation from K Monel	22
Figure 3	Gamma Energy from Absorption Measurements	22
Figure A1	Gamma Decay of Armco Iron and Duriron	34
Figure A2	Gamma Decay of 1015, 1030, 1045 and 6150 Iron Alloys	35
Figure A3	Gamma Decay of Nickel, K Monel and Hastelloys	36
Figure A4	Gamma Decay of Inconel and Inconel X	37
Figure A5	Gamma Decay of Carpenter 20 Steel	38
Figure A6	Gamma Decay of 302, 303, 309, and 317 Steels	39
Figure A7	Gamma Decay of 304 Steel	40
Figure A8	Gamma Decay of 310 Steel	41
Figure A9	Gamma Decay of 316 Steel	42
Figure A10	Gamma Decay of 347 Steel	43
Figure A11	Gamma Decay of 405 Steel	44
Figure A12	Gamma Decay of 410, 414, 431, 502 Steels	45
Figure A13	Gamma Decay of 430 Steel	46
Figure A14	Gamma Decay of 446 Steel	47
Figure A15	Gamma Decay of 2S Aluminum and Beryllium	48
Figure A16	Gamma Decay of 3S and 52S Aluminum	49
Figure A17	Gamma Decay of 72S Aluminum and Titanium	50
Figure A18	Gamma Decay of Cadmium	51
Figure A19	Gamma Decay of Copper	52
Figure A20	Gamma Decay of Lead	53
Figure A21	Gamma Decay of Niobium	54
Figure A22	Gamma Decay of Thorium	55
Figure A23	Gamma Decay of Zirconium, Tungsten Steel	56
Figure A24	Gamma Decay of Barytes Concrete	57
Figure A25	Gamma Decay of Brookhaven Cement	58
Figure A26	Gamma Decay of Portland Concrete	59
Figure A27	Gamma Decay of GBF Graphite	60
Figure A28	Gamma Decay of CS Graphite	61
Figure A29	Gamma Decay of C18 Graphite	62

INTRODUCTION

The activity induced in materials exposed to neutrons may be calculated from the flux and the energy distribution of neutrons, the chemical composition including trace elements, and the isotopic activation cross sections for the nuclear reactions as a function of energy. The problem is simplified if results are desired only to an order of magnitude so that these physical parameters may be approximated. If some of the components of the material have large cross sections for thermal neutrons, and the radioactive products from these reactions have long half lives, only these need be considered, since in this case contributions from trace elements will be insignificant.

If trace elements contribute significantly to the activity, it may be necessary to measure the induced radiation experimentally. In many cases a measurement of induced activity is more sensitive than other analytical methods for determination of trace elements. Most often, uncertainty exists in the parameters mentioned above, and it is then necessary to measure the activity experimentally.

Experimentally measured decay curves for about 50 materials, which were irradiated in the isotope stringer of the ORNL Graphite Reactor, are here analyzed into the component activities in order that the induced activity for any exposure period and decay time may be readily calculated. If materials are activated by exposure to a higher ratio of fast to thermal neutrons than was present in this instance (n, p) and (n,α) reactions, which are in many cases more predominant with fast neutrons, are likely to give relatively greater contribution.

The composition of trace elements in similar materials will likely be different from this specific sampling; however, this sampling should prove useful as an indication of order of magnitude. This should be true in particular in the instances where a number of related alloys have been examined.

After a material is removed from the reactor a short cooling-off period will allow short-lived activities to decay; therefore, interest here is centered in long-lived activities. The sensitivity of determining long-lived activities is greatest for long periods of exposure in the reactor. The exposure periods given here ranged from one month to two years. After a six month exposure period all activities with half lives of less than a month are nearly saturated so that only longer half lives continue to build up. Since the long-lived activities may mask the short-lived activities, the sensitivity of measurement of the short-lived activities in many instances is less for the six month period than for an exposure period of a few hours.

Table I is an index of the decay curves. Nominal compositions of the materials are listed here also. In Table II are listed saturated values of the component activities which were determined from analysis of the decay curves as will be described later. Handbook values of the thermal neutron cross sections of the elements which are components of the materials are listed in Table III. Ion chamber responses for other disintegrations relative to the response for a photon of the average energy of the photons emitted by Co^{60} (which was used to calibrate the ion chamber) are given in Table IV. In Table V the value of activity calculated from the values of Tables III and IV is compared with the experimentally measured values. Half thickness of lead values for absorption of the radiation are listed in Table VI.

Table I

Index to Decay Curves and Nominal Composition of Materials

Material	Figure	Nominal Composition
Iron Alloys		
Iron	A1	Armco Ingot Iron
Duriron	A1	Fe; 0.80 C; 14.5 Si, 0.35 Mn
1015	A2	Fe; 0.70/1.00 Mn; 0.13/0.18 C; 0.040 max P; 0.050 max S
1030	A2	Fe; 0.60/0.90 Mn; 0.28/0.34 C; 0.040 max P; 0.050 max S
1045	A2	Fe; 0.60/0.90 Mn; 0.43/0.50 C; 0.040 max P; 0.050 max S
6150	A2	Fe; 0.65/0.90 Mn; 0.80/1.10 Cr; 0.20/0.35 Si; 0.040 max P; 0.040 max S
Nickel Alloys		
Nickel	A3	99+ Ni; (0.014 Co by chemical analysis)
Hastelloy A	A3	Ni; 17/21 Mo; 17/21 Fe
Hastelloy B	A3	Ni; 24/32 Mo; 3/7 Fe; 0.02/0.12 C
Hastelloy C	A3	Ni; 14/19 Mo; 4/8 Fe; 0.04/0.05 C; 12/16 Cr; 3/5.5 W (0.05 Co by chemical analysis)
Hastelloy D	A3	Ni; 8/11 Si; 2/5 Cu; 1 max Al
Inconel	A4	79.5 Ni; 13 Cr; 6.5 Fe; 0.08 C; 0.2 Cu; 0.25 Mn
Inconel X	A4	73.0 Ni; 15 Cr; 7.0 Fe; 0.04 C; 0.7 Al; 0.50 Mn; 0.40 Si; 1.0 Nb; 2.5 Ti
K Monel	A3	66 Ni; 30 Cu; 3 Al
Stainless Steels		
Carpenter 20	A5	Fe; 20.0 Cr; 29.0 Ni; 0.07 max C; 2.0 min Mo; 3.0 min Cu
302	A6	Fe; 17/19 Cr; 8/10 Ni; 0.08/0.15 C
303	A6	Fe; 17/19 Cr; 8/10 Ni; 0.15 max C
304	A7	Fe; 18/20 Cr; 8/11 Ni; 0.08 max C
309 SCb	A6	Fe; 22/24 Cr; 12/15 Ni; Nb (Cb) added for stabilization
310	A8	Fe; 24/26 Cr; 19/22 Ni; 0.25 max C
316	A9	Fe; 16/18 Cr; 10/14 Ni; 0.1 max C
317	A6	Fe; 18/20 Cr; 11/14 Ni; 3/4 Mo; 0.1 max C
347	A10	Fe; 17/19 Cr; 9/12 Ni; 10 x C min Nb
405	A11	Fe; 11/13.5 Cr; 0.08 max C; 0.1/0.3 Al
410	A12	Fe; 11.5/13.5 Cr; 0.15 max C (0.017 Co by chemical analysis)
414	A12	Fe; 11.5/13.5 Cr; 1.25/2.5 Ni; 0.15 max C
430	A13	Fe; 14/18 Cr; 0.12 max C; (0.027 Co by chemical analysis)
431	A12	Fe; 15/17 Cr; 1.25/2.5 Ni; 0.2 max C
446	A14	Fe; 23/27 Cr; 0.35 max C; 0.25 max N
502	A12	Fe; 4/6 Cr; 0.1 max C
Aluminum Alloys (Alcoa)		
2S	A15	99 min Al
3S	A16	Al; 1.2 Mn
52S	A16	Al; 2.5 Mg; 0.25 Cr
72S	A17	Al; 1.0 Zn

Table I (Cont.)

Index to Decay Curves and Nominal Composition of Materials

Material	Figure	Nominal Composition
Other Metals		
Beryllium	A15	
Cadmium	A18	
Copper	A19	
Lead	A20	
Niobium	A21	
Titanium	A17	
Thorium	A22	
Ferro-tungsten Alloy	A23	63.97 Fe; 35.27 W; 0.47 Mn (by chemical analysis)
Zirconium	A23	
Concrete		
Barytes Concrete, Batch 147	A24	9.6 portland cement, type 1; 46.0 barytes, coarse(1); 40.0 barytes, fine(2); 4.4 water
Brookhaven Cement, Batch 145	A25	29.1 portland cement, type 1; 58.2 limonite; 12.7 water
Portland Concrete, Batch 146	A26	10.4 portland cement, type 1; 56.0 rock; 25.5 sand; 8.1 water
Graphite		
GBF Graphite	A27	National Carbon Company designation GBF (Gas-baked and highly refined)
CS Graphite	A28	National Carbon Company designation CS
C18 Graphite	A29	National Carbon Company designation C-18

(1) Composition of barytes, coarse: 56.4 Ba; 39.4 SO_4; 0.5 Ca; 1.00 Fe; 0.31 Si 0.15 Na; 0.08 Al; 0.01 Mg; 0.02 Mn; $<$0.3 Zn

(2) Composition of barytes, fine: 47.7 Ba; 33.9 SO_4; 0.9 Ca; 9.8 Fe; 1.00 Si; 0.15 Na; 0.3 Al; 0.3 Mg; 0.08 Mn; 0.3 Zn

RESULTS

Analysis of Decay Curves

The activity induced in each component isotope increases with the irradiation time until the rate of decay of radioactive atoms approaches the rate of formation. At this time the activity is termed saturated. In general the irradiation time for the materials whose decay curves are shown in the Appendix was not long enough for the activities to reach saturation. A different decay curve is then obtained for each irradiation time. To aid in the calculation of a decay curve for any desired irradiation time, the decay curves were analyzed and saturated values for the component activities were calculated. These are listed in Table II. The method by which these values were obtained is as follows.

When a material is removed from the reactor the value of each component of the activity is given as a function of time by

$$A_t = A_i \exp(-0.693\, t_d/t_{\frac{1}{2}}) \qquad \text{equation 1}$$

where t_d = the decay time

$t_{\frac{1}{2}}$ = the half life

A_i = the induced activity for zero decay time

A_t = the activity at decay time t

By equation 1 a linear plot is given by the logarithm of the activity of the component versus decay time. This is the basis for the following procedure:

Plot the logarithm of the activity versus the decay time. Draw a tangent to the curve in the region with the greatest decay time. This is a first approximation to the component activity with the longest half life. Subtract this component from the total curve and draw a tangent to the resulting curve. If this second component is appreciable in the region that was used in the determination of the first component, it is necessary to repeat the determination for the

first component, this time first subtracting out the second component from the total curve. The process is continued until linear components are obtained which add to give the total curve.

The saturated values of the component activities are calculated from the relations:

$$A_s = A_i/X_s \qquad \text{equation 2}$$

$$X_s = 1 - \exp(-0.693\ t_i/t_{\frac{1}{2}}) \qquad \text{equation 3}$$

where A_s = the saturated value of the component activity

A_i = the activity at irradiation time t_i and zero decay time

t_i = the irradiation time

$t_{\frac{1}{2}}$ = the half life of the component activity

X_s = the saturation factor

A decay curve for any desired irradiation time may be constructed by the following procedure:

Determine A_i for each component using eq 2 and values of A_s from Table II. Plot the logarithm of the activity versus the decay time (a straight line) for each component. Add the curves for the components to get the total curve for the material.

The method employed to break down the decay curve into components lumps together all activities with long half lives so that extrapolation of the data is not accurate to irradiation times long enough for part of this lumped value to approach saturation.

An example of a typical decay curve analysis is presented in Figure 1 which shows the component activities for 347 steel. A tabulation of the parameters follows:

$t_{\frac{1}{2}}$	A_s (from Table II)	X_s (for 1170 hours irradiation)	A_i (for 1170 hours irradiation)
25d	3.2×10^7	0.741	2.2×10^7
45d	3.0×10^7	0.528	1.6×10^7
120d	3.2×10^7	0.246	7.9×10^6
5.3y	7.4×10^8	0.0173	1.3×10^7

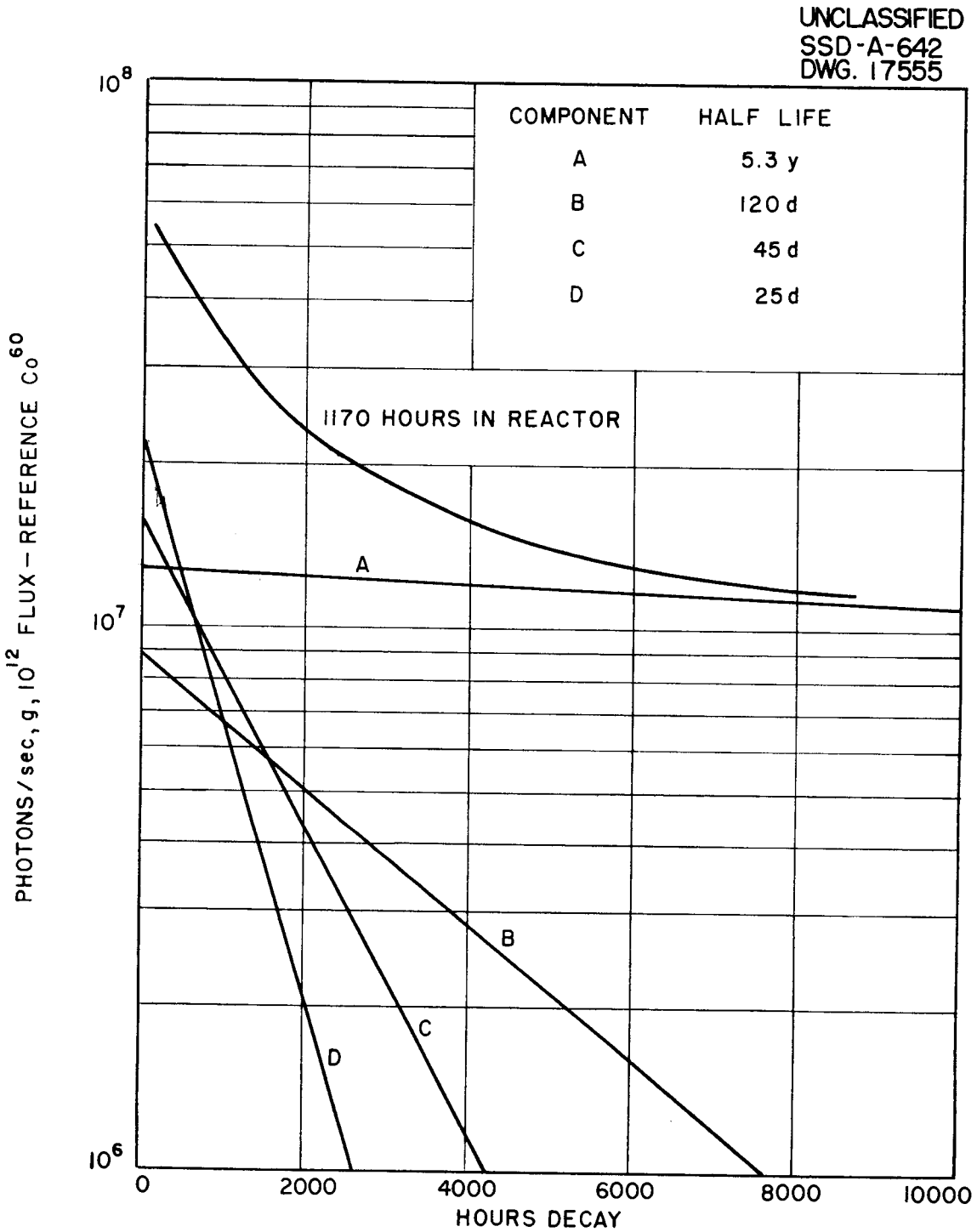

Fig. 1 – Analysis of Decay Curve for 347 Steel

UNCLASSIFIED
DWG. 17586

Table II

Saturated Values of the Component Activities of the Decay Curves, Equivalent Co^{60} Photons*/(sec, gm, 10^{12} flux)

Material	Irradiation Period, hours	Component 1		Component 2		Component 3		Component 4		Component 5	
		Half Life	Activity	Half Life	Activity	Half Life	Activity	Half Life	Activity	Half Life	Activity
Iron Alloys											
Armco Iron	4870	2.5h	9×10^7	45d	3.5×10^7	5.3y	5.7×10^7				
Duriron	5050	2.5h	1.3×10^9	45d	2.9×10^7	5.3y	7.3×10^7				
1015	4700	2.5h	1.5×10^9	45d	3.7×10^7	5.3y	5.3×10^7				
1030	4700	2.5h	1.5×10^9	45d	3.7×10^7	5.3y	5.3×10^7				
1045	4700	2.5h	1.8×10^9	45d	3.7×10^7	5.3y	9.0×10^7				
6150	4700	2.5h	1.5×10^9	45d	3.7×10^7	5.3y	5.3×10^7				
Nickel Alloys											
Nickel	5050	2.5h	3×10^7	60d	4.4×10^7	5.3y	9.1×10^8				
Hastelloy A	4680	2.5h	1.1×10^9	60h	6×10^7	60d	4×10^7	5.3y	4.1×10^9		
Hastelloy B	4680	2.5h	1.5×10^9	60h	5×10^7	60d	2.5×10^7	5.3y	3.1×10^9		
Hastelloy C	4680	2.5h	3.6×10^9	60h	2×10^7	25d	3.1×10^7	60 d	1×10^8	5.3y	1.1×10^9
Hastelloy D	4680	2.5h	1.5×10^9	13h	3.0×10^8	60d	4.4×10^7	5.3y	4.4×10^9		
Inconel	1850	2.5h	3.5×10^8	25d	1.5×10^7	60d	4.9×10^7	5.3y	8.5×10^8		
Inconel	4370	2.5h	3.5×10^8	decay time too short for analysis of these components							
Inconel X	1850	2.5h	7×10^8	25d	2×10^7	60d	$5.x 10^7$	115d	1.1×10^8	5.3y	8×10^8
Inconel X	4370	2.5h	7×10^8	decay time too short							
K Monel	4700	2.5h	2×10^9	13h	1.6×10^9	60d	3.1×10^7	5.3y	2.4×10^9		
Stainless Steels											
Carpenter 20	1170	2.5h	2.0×10^9	15h	1.7×10^8	25d	2.5×10^7	45d	4.2×10^7	5.3y	1.5×10^9
Carpenter 20	4380	2.5h	1.5×10^9	15h	1.1×10^8	25d	1.6×10^7	45d	4.5×10^7	5.3y	1.4×10^9
302	4700	2.5h	1.4×10^9	25d	2.7×10^7	45d	4.0×10^7	5.3y	7.1×10^8		
303	4540	2.5h	9×10^8	25d	2.7×10^7	45d	4.0×10^7	5.3y	6.9×10^8		
304	1170	2.5h	8×10^8	25d	2.0×10^7	45d	4.0×10^7	5.3y	6.3×10^8		
304	4380	2.5h	9×10^8	25d	2.0×10^7	45d	4.0×10^7	5.3y	5.7×10^8		
309	4540	2.5h	3.2×10^9	25d	3×10^7	45d	4×10^7	120d	4×10^7	5.3y	9.5×10^8

UNCLASSIFIED
DWG. 17587

Table II (Cont.)

Saturated Values of the Component Activities of the Decay Curves, Equivalent Co^{60} Photons*/(sec, gm, 10^{12} flux)

Material	Irradiation Period, hours	Component 1		Component 2		Component 3		Component 4		Component 5	
		Half Life	Activity	Half Life	Activity	Half Life	Activity	Half Life	Activity	Half Life	Activity
310	1170	2.5h	3×10^9	25d	3.6×10^7	45d	4.2×10^7	5.3y	1.2×10^9		
310	4500	2.5h	4×10^9	25d	3.6×10^7	45d	4.2×10^7	5.3y	1.3×10^9		
316	1170	2.5h	2.5×10^9	25d	2.8×10^7	45d	3.6×10^7	5.3y	8.1×10^8		
316	4500	2.5h	4.5×10^9	25d	3.5×10^7	45d	3.7×10^7	5.3y	8.3×10^8		
317	4700	2.5h	4.5×10^9	25d	3.5×10^7	45d	4.0×10^7	5.3y	1.1×10^9		
347	1170	2.5h	2.1×10^9	25d	3.2×10^7	45d	3.0×10^7	120d	3.2×10^7	5.3y	7.4×10^8
347	4500	2.5h	3.1×10^9	25d	3.7×10^7	45d	3.0×10^7	120d	3.3×10^7	5.3y	7.0×10^8
405	1170	2.5h	7×10^8	25d	2.3×10^7	45d	3.4×10^7	5.3y	1.6×10^8		
405	4500	2.5h	1.1×10^9	25d	2.4×10^7	45d	3.7×10^7	5.3y	1.6×10^8		
410	4870	2.5h	1.0×10^9	25d	2.0×10^7	45d	3.9×10^7	5.3y	1.5×10^8		
414	4540	2.5h	1.0×10^9	25d	2.0×10^7	45d	3.5×10^7	5.3y	2.2×10^8		
430	1170	2.5h	7×10^8	25d	2.5×10^7	45d	3.2×10^7	5.3y	1.5×10^8		
430	4280	2.5h	8×10^8	25d	2.8×10^7	45d	2.8×10^7	5.3y	1.3×10^8		
431	4540	2.5h	1.1×10^9	25d	2.1×10^7	45d	3.9×10^7	5.3y	2.4×10^8		
446	1170	2.5h	1.1×10^9	25d	4.6×10^7	45d	2.8×10^7	5.3y	1.8×10^8		
446	4380	2.5h	1.3×10^9	25d	4.3×10^7	45d	2.7×10^7	5.3y	1.6×10^8		
502	4510	2.5h	4.6×10^8	25d	6×10^6	45d	3.5×10^7	5.3y	6.8×10^7		
Aluminum Alloys											
2S	15380	2.5h	$\sim 2 \times 10^8$	15h	1.2×10^7	130d	1.3×10^5	5.3y	5.7×10^5		
3S	4510	2.5h	1.3×10^9	15h	8.2×10^6	45d	2.3×10^5	5.3y	1.6×10^6		
52S	4510	2.5h	7×10^6	15h	8.2×10^6	120d	3.6×10^5	5.3y	4×10^5		
72S	4870	2.5h	$< 10^7$	15h	1.4×10^7	250d	1.4×10^7				
Other Metals											
Beryllium	12170	2.5h	8×10^6	80d	1.2×10^6	5.3y	1.9×10^6				
Cadmium	1850	2.5h	none	60h	2.3×10^8	40d	2.4×10^6	250d	1.8×10^6		
	4370	2.5h	none	60h	2.3×10^8	40d	2.4×10^6	250d	1.8×10^6		
Copper	4370	2.5h	1×10^9	13h	4.2×10^9	> 100d	2×10^6				

Table II (Cont.)

Saturated Values of the Component Activities of the Decay Curves, Equivalent Co^{60} Photons*/(sec, [redacted], 10^{12} flux)

Material	Irradiation Period, hours	Component 1		Component 2		Component 3		Component 4		Component 5	
		Half Life	Activity	Half Life	Activity	Half Life	Activity	Half Life	Activity	Half Life	Activity
Lead	4370	2.5h	$< 10^5$	20-70h	4×10^5	140d	6.4×10^5				
Niobium	5050	2.5h	none	115d	7.5×10^8						
Titanium	4870	2.5h	5×10^7	35h	2.5×10^6	80d	1.4×10^6				
Thorium	670	2.5h	none	27d	3.5×10^9						
Thorium	4370			27d	3.2×10^9						
Ferro-tungsten	5050	2.5h	1.5×10^9	20h	1.7×10^7	45d	3.5×10^7	5.3y	3.2×10^7		
Zirconium	4700	2.5h	3×10^8	20h	8×10^7	60d	4.0×10^8				
Concrete											
Barytes Concrete	160	2.5h	not measured	12d	1.2×10^7	60d	4×10^6	250d	2.3×10^7	5.3y	5×10^6
	680	2.5h	9×10^7	12d	1.2×10^7	60d	3×10^6	250d	2.2×10^7	5.3y	4×10^6
	4370	2.5h	1.0×10^8	12d	1×10^7	60d	3×10^6	250d	2×10^7	5.3y	5×10^6
Brookhaven Cement	160	2.5h	not measured	15h	not measured	50d	1.5×10^7	250d	1.7×10^6	5.3y	1.7×10^7
	680	2.5h	9×10^8	15h	2×10^7	50d	1.3×10^7	250d	1.7×10^6	5.3y	1.3×10^7
	4370	2.5h	1.0×10^9	15h	3×10^7	50d	1.6×10^7	250d	1.7×10^6	5.3y	1.3×10^7
Portland Concrete	160	2.5h	not measured	15h	not measured	12d	1.1×10^6	85d	2.0×10^6	5.3y	6×10^6
	680	2.5h	9×10^7	15h	8×10^7	12d	9×10^5	85d	2.0×10^6	5.3y	5×10^6
	4370	2.5h	1.0×10^8	15h	9×10^7	12d	9×10^5	85d	2.5×10^6	5.3y	5×10^6
Graphite GBF	310	2.5h	none	15h	4×10^4	too weak to measure					
	640	2.5h	none	15h	2×10^4	too weak to measure					
	1360	2.5h	none	15h	1×10^5	100d	8.0×10^2	5.3y	1.2×10^4		
CS	310	2.5h	none	15h	5.0×10^4	35h	1.5×10^4	85d	1.6×10^4	5.3y	4.0×10^4
	640	2.5h	none	15h	2.5×10^4	35h	1.4×10^4	85d	1.9×10^4	5.3y	4.9×10^4
	1360	2.5h	none	15h	1×10^5	35h	2×10^4	85d	1.6×10^4	5.3y	5.0×10^4
C-18	15400	2.5h	none	15h	7×10^5	70d	1.3×10^5	5.3y	8.3×10^5		

*See page 31 for the method of calibration of the ion chamber

Calculation of Activity

If the required factors are known, A_s, the saturated activity defined by equation 2, may be estimated for each component from the equation

$$A_s = \sigma NR \times 10^{12} \qquad \text{equation 4}$$

where A_s = the saturated activity based on one gram of element and 10^{12} flux; equivalent Co^{60} photons*/(sec, gm, 10^{12} flux)

σ = the isotopic thermal neutron cross section; sq. cm.

N = the atoms of reacting isotope per gram of material

R = the ratio of the ion chamber response for a disintegration of the radioactive isotope to the response for a photon of the average energy of those emitted by Co^{60} (1.25 Mev)

For example, to calculate the 2.59 h activity induced in one gram of Mn. First σN is calculated (Table III)

$$\sigma N = (\sigma AF/M) = (12 \times 10^{-24} \times 0.603 \times 10^{24} \times 1/55) = 0.13 \text{ sq cm/gm Mn}$$

where σ = the isotopic cross section for $Mn^{55}(n, \gamma)Mn^{56}$ = 12 barns = 12×10^{-24} sq cm

A = the number of atoms/mole, Avogadro's number = 0.603×10^{24}

F = the natural isotopic abundance expressed as fraction of total number of atoms = 1.00 for Mn^{55}

M = the chemical molecular weight = 55 gm Mn/mole

The ion chamber response (Table IV* is calculated as the sum of the responses for the photons emitted by Mn^{56}

$$R = \sum_{1}^{N} P(E_i)R(E_i)/100 = (100 \times 0.80 + 25 \times 1.25 + 15 \times 1.34)/100 = 1.32$$

*The method by which the ionization chamber was calibrated is described on p. 31

where R = the response for the isotope relative to a Co^{60} photon (1.25 Mev)

$R(E_i)$ = the relative response for the photon with energy E_i emitted in the decay of the isotope

$P(E_i)$ = the percentage of disintegrations for which the photon with energy E_i is emitted

N = the number of different energies of photons emitted in the decay of the isotope

Substituting in equation 4 gives the "calculated" activity listed for Mn in Table V.

$$A_s = \sigma NR \times 10^{12} = 0.13 \times 1.32 \times 10^{12} = 1.7 \times 10^{11} \text{ equivalent } Co^{60} \text{ photons/ (sec, gm, } 10^{12} \text{ flux)}$$

The "measured" activity listed in Table V is the quotient of the saturated value of the 2.59 hour component activity in Inconel X and the fraction of Mn in Inconel X as listed in Table I.

Absorption Measurements

Absorption measurements were made by interposing sheets of lead between the materials and a Geiger tube. A typical absorption curve is shown in Figure 2 where the experimental points for K monel are shown. The curve of Figure 2 is the sum of the curves shown for the component activities which were calculated starting with the saturated component activities listed in Table II. The calculation is shown in the following tabulation:

Half Life $t_{\frac{1}{2}}$	(1) Activity of Saturated Component, A_i	(2) Saturation Factor for a 4700 Hour Exposure, X_s	(3) Fraction of Activity Remaining after 30 Hours Decay	Activity after 4700 Hours Exposure and 30 Hours Decay = (1) x (2) x (3)	Percentage of Total	
2.5h	2×10^9	1.0	0.0002	0		
13h	1.6×10^9	1.0	0.20	3.2×10^8		63
60d	3.1×10^7	0.895	1.0	0.3×10^8	6	37
5.3y	2.4×10^9	0.0678	1.0	1.6×10^8	31	

Table III

Product of the Cross Section and the Number of Target Atoms per Gram of Element, σN

Target Isotope	Half Life of Radioactive Product	Isotopic Activation Cross Section*, 10^{-24} sq cm	Abundance, mole per cent	Chemical Atomic Weight, gms/mole	σN sq cm/gm
Ti^{50}	72d	0.039	5.3	47.9	2.6×10^{-5}
Cr^{50}	26.5d	16	4.1	52	7.6×10^{-3}
Mn^{55}	2.59h	12	100	55	0.13
Fe^{58}	46.d	0.8	0.33	56	2.8×10^{-5}
Co^{59}	5.3y	34	100	59	0.35
Ni^{64}	2.56h	3.0	1	58.7	3.1×10^{-4}
Cu^{63}	12.9h	4.3	69	63.5	0.028
Zn^{64}	250d	0.5	48.9	65	2.3×10^{-3}
Zr^{94}	65d	0.43	17.4	91.2	4.9×10^{-4}
Zr^{96}	17h	0.29	2.8	91.2	5.4×10^{-5}
Mo^{98}	67h	0.4	23.9	96.0	6×10^{-4}
Cd^{114}	58h	1.1	28.8	112.4	1.7×10^{-3}
Cd^{114}	43d	0.14	28.8	112.4	2.2×10^{-4}
Ba^{130}	12d	6	0.104	137.4	2.7×10^{-5}
Ta^{181}	113d	21	100	181	7.0×10^{-2}
W^{186}	24h	34	28.7	184	3.2×10^{-2}
Th^{232}	27.4d	6	100	232.1	1.6×10^{-2}

*Taken from (4), p. 31

Table IV

Ion Chamber Responses for Isotopes

Isotope	Half Life	Photon Energies	Relative Ion Chamber Response*	Percentage of Disintegrations Yielding a Photon	Average Relative Response R
Na^{24}	14.8h	1.38 2.75	1.04 1.54	100 100	2.58
Sc^{46}	85d	0.88 1.12	0.84 0.96	100 98	1.80
Cr^{51}	26.5d	0.27 0.32	0.27 0.34	? 3	>0.01
Mn^{56}	2.59h	0.84 1.81 2.13	0.80 1.81 2.13	100 25 15	1.32
Fe^{59}	46d	1.10 1.30	0.94 1.00	50 50	1.00
Co^{60}	5.3y	1.16 1.31	0.96 1.04	100 100	2.00
Ni^{65}	2.56h	1.01 1.49	0.90 1.1	14 ?	>0.13
Cu^{64}	12.9h	0.51	0.51	37	0.19
Zn^{65}	250d	1.12	0.96	46	0.44
Zr^{95}	65d	0.23 0.73 0.92	0.23 0.72 0.84	93 93 7	0.77
Cd^{115}	58h	0.34 0.52	0.34 0.52	? 60	>0.3
Ta^{182}	113d	1.13 1.22	0.96 1.02	37 57	0.92

* Taken from (1), p. 31

Table V

Calculated and Measured Values of Induced Activity

Reaction	σN (Table III)	Relative Ion Chamber Response Disintegration (Table IV)	Calculated Activity = σN x Ion Chamber Response x 10^{12} flux, equivalent Co^{60} photons/(sec, gm, 10^{12} flux)	Measured Activity from Table II Divided by the Fractional Composition of the Reacting Element
$Al^{27}(n,\alpha)Na^{24}$	---	2.58	---	1.2×10^{7} (from 2S aluminum)
$Ti^{46}(n,p)Sc^{46}$	---	1.80	---	1.4×10^{6} (from both reactions on titanium)
$Ti^{50}(n,\gamma)Ti^{51}$	2.6×10^{-5}	----	---	
$Cr^{50}(n,\gamma)Cr^{51}$	7.6×10^{-3}	>0.01	$> 8 \times 10^{7}$	1.4×10^{8} (from 310 SS)
$Mn^{55}(n,\gamma)Mn^{56}$	0.13	1.32	1.7×10^{11}	1.4×10^{11} (from inconel)
$Fe^{58}(n,\gamma)Fe^{59}$	2.8×10^{-5}	1.00	2.8×10^{7}	3.7×10^{7} (from 1015 iron)
$Co^{59}(n,\gamma)Co^{60}$	0.35	2.00	7.0×10^{11}	7.8×10^{11} (from electrolytic cobalt)
$Ni^{58}(n,p)Co^{58}$	---		---	4.4×10^{7} (from nickel)
$Ni^{60}(n,p)Co^{60}$	---	2.00	---	8.6×10^{8} (from nickel)
$Ni^{64}(n,\gamma)Ni^{65}$	3.1×10^{-4}	>0.13	$> 8 \times 10^{7}$	$< 3 \times 10^{7}$ (from nickel)
$Cu^{63}(n,\gamma)Cu^{64}$	0.028	0.19	5.3×10^{9}	4.2×10^{9} (from copper)
$Zn^{64}(n,\gamma)Zn^{65}$	2.3×10^{-3}	0.44	1.0×10^{9}	1×10^{9} (from 72S aluminum)
$Zr^{94}(n,\gamma)Zr^{95}$	4.9×10^{-4}	0.77	3.8×10^{8}	4×10^{8} (from zirconium)
$Zr^{96}(n,\gamma)Zr^{97}$	5.4×10^{-5}	---	---	8×10^{7} (from zirconium)
$Mo^{98}(n,\gamma)Mo^{99}$	6×10^{-4}	---	---	2×10^{8} (from Hastelloy B)
$Cd^{114}(n,\gamma)58hCd^{115}$	1.7×10^{-3}	>0.3	$> 5 \times 10^{8}$	2.3×10^{8} (from cadmium)
$Cd^{114}(n,\gamma)43dCd^{115}$	2.2×10^{-4}	---	---	2.4×10^{6} (from cadmium)
$Ba^{130}(n,\gamma)Ba^{131}$	2.7×10^{-5}	---	---	2.7×10^{7} (from barytes concrete)
$Ta^{181}(n,\gamma)Ta^{182}$	7.0×10^{-2}	0.92	6.4×10^{10}	---
$W^{186}(n,\gamma)W^{187}$	3.2×10^{-2}	---	---	4.8×10^{7} (from ferrotungsten alloy)
$Th^{232}(n,\gamma)Th^{233}$	1.6×10^{-2}	---	---	3.5×10^{9} (from thorium)

The 13h component is identified as Cu^{64}; the 5.3y component, as Co^{60}. Absorption curves of the components were plotted in Figure 2 from the above percentages and the half thicknesses for radiation from Cu^{64} and Co^{60} taken from Figure 3. The 60 day component is from the Ni^{58} (n,p) Co^{58} reaction and can be lumped with the 5.3y component since it is relatively small.

Scattering of experimental points prevents resolution of the total curve of Figure 2 into components directly as the decay curves were resolved. Only for isotopes with more widely differing absorption half thicknesses is resolution possible. In this instance the components merge to give for the total curve a half thickness of 0.34 in. of lead which is only a little lower than the average of the component curves; 0.63 x 0.28 in. + 0.37 x 0.56 in. = 0.37 in. Figure 3 is a plot of half thickness versus energy for the materials measured whose composition and decay schemes are known. The above example illustrates how rough values for the average energy of materials of unknown composition may be estimated from Figure 3; in this case the 0.34 in. value of half thickness gives an average energy of 0.65 Mev, a value between Cu^{64} and Co^{60}.

Table VII lists the half thicknesses of all the materials measured. Where it is possible to resolve the curve into components, this is done. The percentage figures for the components refer to percentage of the ion chamber response.

UNCLASSIFIED
SSD-A-643
DWG. 17556

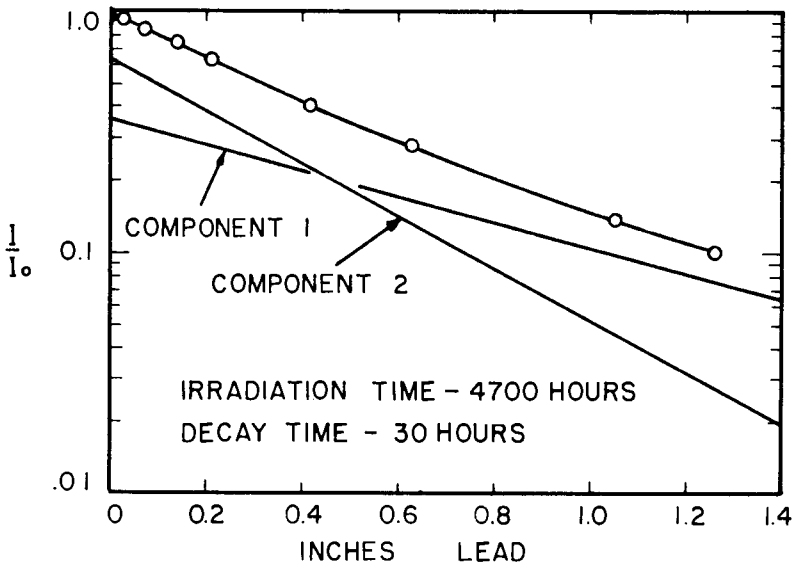

	HALF THICKNESS
COMPONENT 1	0.56
COMPONENT 2	0.28
TOTAL CURVE	0.34

Fig. 2 — Absorption of Gamma Radiation from K Monel

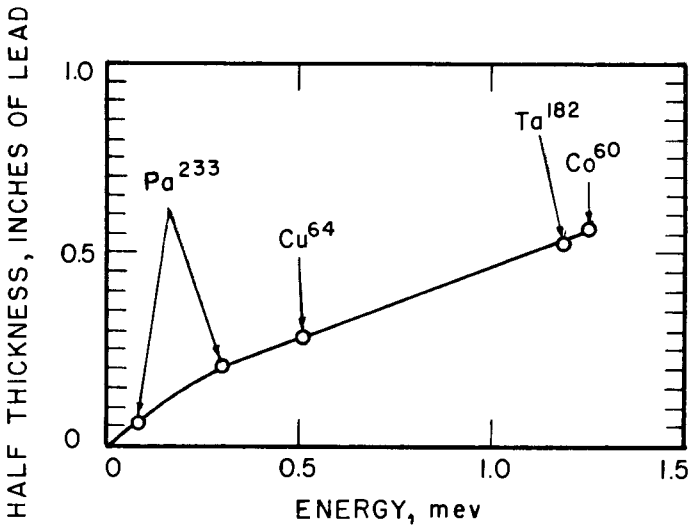

Fig. 3 – Gamma Energy from Absorption Measurements

Table VI

Absorption of Gamma Radiation

Material	Irradiation Period, hours	Decay Time, hours	Half Thickness, inches of lead
Iron Alloys			
Iron (Armco)	4870	31	0.54
	4870	10,000	0.56
Duriron	5050	27	0.53
1015	4700	29	0.53
1030	4700	29	0.53
1045	4700	28	0.53
6150	4700	28	0.53
Nickel Alloys			
Nickel	5050	27	0.49
Nickel	5050	9,600	0.56
Hastelloy A	4680	600	0.59
" "	4680	9,100	0.56
Hastelloy B	4680	600	0.59
Hastelloy C	4680	600	0.59
Hastelloy D	4680	600	0.61
Inconel	1850	530	0.51
Inconel	1850	4,800	0.54
Inconel	4370	770	0.54
Inconel X	1850	530	0.53
Inconel X	4370	790	0.54
K Monel	4700	720	~ 0.34
K Monel	4700	10,100	0.56
Stainless Steels			
Carpenter 20	1170	100	0.52
Carpenter 20	4380	80	0.54
302	4700	27	0.49
303	4540	27	0.54
304	4380	100	0.47
309	4540	31	0.52
310	1170	100	0.48
310	4500	80	0.51
316	1170	100	0.45
316	4500	80	0.54
317	4700	27	0.51
347	1170	100	0.49
347	4500	80	0.54
405	1170	100	0.49
405	4500	80	0.52
410	4870	27	0.53
414	4540	28	0.54
430	1170	100	0.45
430	4280	80	0.53
431	4540	28	0.50
446	1170	100	0.47
446	4280	80	0.49
502	4510	30	0.51

Table VI (Cont.)

Absorption of Gamma Radiation

Material	Irradiation Period, hours	Decay Time, hours	Half Thickness, inches of lead
Aluminum Alloys			
2S	15380	2,200	0.49
2S	15380	12,400	0.57
3S	4510	27	0.50
3S	4510	11,700	0.57
52S	4510	27	0.56
52S	4510	11,500	0.54
72S	4870	33	0.51
72S	4870	10,800	0.53
Other Metals			
Cadmium	1850	530	0.37
Cadmium	4370	32	0.24
Cadmium	4370	2,200	0.48
Copper	4370	28	0.28
Copper	4370	2,200	0.49
Lead	4370	27	0.45
Lead	4370	2,070	0.45
Niobium	5050	27	0.52
Niobium	5050	9,650	0.51
Titanium	4870	28	0.42
Titanium	4870	10,800	0.44
Thorium	670	29	70% 0.21
			30% 0.05
Ferro-tungsten	5050	28	0.48
Zirconium	4700	28	0.28
Zirconium	4700	1,020	0.34
Beryllium	12170	24	0.45
Beryllium	12170	500	0.47
Beryllium	12170	19,300	0.57
Concrete			
Barytes Concrete	680	2,700	0.52
" "	4370	220	0.42
	4370	13,700	0.48
Brookhaven Cement	680	2,700	0.58
	4370	200	0.50
	4370	13,700	0.50
Portland Concrete	680	2,700	0.48
	4370	220	0.46
	4370	13,700	0.50

Table VI (Cont.)

Absorption of Gamma Radiation

Material	Irradiation Period, hours	Decay Time, hours	Half Thickness, inches of lead
Graphite			
GBF	644	24	0.54
	644	100	0.45
	1850	100	0.45
	1360	15,140	0.50
CS	644	24	0.54
	644	100	0.45
	1850	100	0.47
	1360	15,140	0.59
C-18	15400	100	0.46
	15400	2,200	0.46
	15400	12,480	0.52

DISCUSSION

Thermal neutron cross sections are used for the (n, γ) reaction calculations, and activation which takes place with neutrons of greater than thermal energy is neglected. The relatively large number of thermal neutrons in comparison with those of higher energy plus the fact that the cross section varies as 1/V make this a good approximation for (n, γ) reactions.

Reactions in which charged particles are emitted by the nucleus, (n, p) and (n, α) reactions, are highly dependent upon the energy of the neutrons, and both cross-section versus energy and flux versus energy functions must be taken into account. Activity measurements listed here are for exposures in the isotope stringer of the X-reactor. Comparison of the flux versus energy function of the X-reactor (3) with a new flux versus energy function should make possible, however, predictions of induced activity for the new flux-energy function for elements whose cross sections are known as a function of energy.

Iron Alloys

The 2.5-hour component may be due both to the $Fe^{56}(n,p)Mn^{56}$ and the $Mn^{55}(n,\gamma)Mn^{56}$ reactions. An upper limit on the (n,p) reaction is fixed by the lowest value of the 2.5-hour component measured for any of the iron alloys. The 2.5-hour component is lowest for Armco iron due to the low manganese content of this iron alloy; the high values for the other iron alloys are due to their maganese content. The 46-day component checks closely for all the iron alloys and is 50% higher than the value calculated for the $Fe^{58}(n,\gamma)$ reaction in Table V. This difference may be due to error introduced by the use of the thermal neutron cross section as an approximation to the cross section for the neutrons with the energy distribution present in the reactor.

The activity component with the longest half life was taken as 5.3 year Co^{60} and is accounted for by a cobalt content of the iron alloys from 0.01 to 0.05%. In 410 and 430 steels, which are steels containing iron, chromium, and manganese, the presence of enough cobalt to account for the 5.3 year activity was confirmed by chemical analysis.

After from 28 to 30 hours decay time, when the ionization chamber current is 80 to 95% due to Fe^{59}, absorption measurements give 1.1 ± 0.1 Mev; after longer decay periods when the proportion of activity from Fe^{59} has decreased and the proportion from Co^{60} has increased, the energy approaches 1.2 ± 0.1 Mev.

Nickel Alloys

Since the 2.5 hour component is only about 10% of the total activity of the nickel sample at the time decay measurements were begun, the accuracy of resolution of this component is not great (about 50%). The activity value calculated for the Ni^{64} (n, γ) reaction does not check the measured value even within this spread, however; the calculated value being about three times too large. It appears that either the cross section or the ion chamber response are given too high a value.

The decay curve of the nickel sample shows a 60-70 day component which is probably from the $Ni^{58}(n,p)Co^{58}$ reaction. In the analysis of the decay curves for nickel-containing stainless steels which have both large 46 day and 5.3 year components resolution of the 60-70 day component from the 46 day component is difficult and for this reason the 60-70 day component is included with the 46 day component, making the 46 day component greater than for iron alloys.

The 5.3 year component activity in nickel-containing materials is in part accounted for by the $Ni^{60}(n,p)Co^{60}$ reaction. The measured value of the activity induced by this reaction was determined from the 5.3 year activity induced in a sample of nickel which contained 0.014% cobalt. This cobalt content accounted for 6% of the 5.3 year component by the Co^{59}(n, γ) reaction; 94% is then due to the Ni^{60}(n,p) reaction. In the other nickel-containing materials - except for inconel and inconel X, which contain even less cobalt than the nickel sample - the 5.3 year activity, after correction for the (n,p) reaction, is equivalent to from 0.1 to 1% cobalt.

After 27 hours decay time the ion chamber response for the nickel sample is about 40% from the 60-70 day component and 60% from the 5.3 year component. The average value of gamma energy is 1.25 Mev for Co^{60} and 0.80 for Co^{58}; this gives an average energy for nickel of 0.4 x 0.80 + 0.6 x 1.25 = 1.07 Mev, in good agreement with the value from absorption measurements, 1.1 ± 0.1 Mev.

Stainless Steels

Activities induced in these alloys are included in the discussion for iron and nickel alloys except for the 26 day and 115 day activities. The 26 day activity is not accurately calculable because of uncertainty as to the exact decay scheme of Cr^{51}. The 115 day activity is due to tantalum present in niobium which has been added to stablize the 309 and 347 alloys.

The 0.3 Mev photons from Cr^{51} account for the low absorption half-thicknesses for the high-chromium steels with 1170 hour exposure time and a few days decay time when the chromium contributes a significant portion of the total induced activity.

Aluminum Alloys

The 15 hour component is due to the $Al^{27}(n,\alpha)Na^{24}$ reaction. The difference in activity values obtained for this reaction for different alloys is attributed to error in resolving this component. The best value is probably given by the 2S alloy since the values of other components are lowest for this material. The 250 day (Zn^{65}) activity induced in 72S aluminum agrees with the calculated value, based on 1% Zn content, within experimental error. The 45 day component in 3S aluminum is probably due to 0.5% iron. The other components of the aluminum alloys could be accounted for by trace elements: 5 ppm tantalum, 1 ppm cobalt. The absorption measurements on the aluminum alloys give energies in agreement with the identity of these activities as Ta^{182} and Co^{60}.

Beryllium

From typical Be analyses it is deduced that the 80 day component is a combination of the activities induced in Zn, Fe, and Ni. It is difficult to resolve

this portion of the curve into more than one component due to the large 5.3 year component which is probably due to a trace of cobalt.

Cadmium

The 58 hour component (Cd^{115}) is less than 1/2 the calculated value. It is likely either that the decay scheme used in Table IV is in error or the cross section of Table III is too high. After 32 hours decay time, when the 60 hour component comprises the major portion of the activity, the energy is about 0.4 Mev, about the average energy of photons from Cd^{115} (see Table IV).

Copper

Since more than 95% of the photons from Cu^{64} result from positron annihilation, the others were neglected in the calculations.

Lead

The portion of the curve from 30-270 hours is extrapolated from the rest of the curve because the electrometer was out of order during this decay period. The energy and half life of the ~130 day component correspond roughly to Ta^{182}.

Niobium

The activity is accounted for by a tantalum content of 1.2%.

Titanium

It is speculated that the approximately 35 hour component is Sc^{48} from the reaction $Ti^{48}(n,p)$. The straightness of the latter part of the decay curve indicates most of the activity is Ti^{51} or Sc^{46} (from $Ti^{46}(n,p)$). The half lives are too nearly the same to distinguish between the Ti^{51} and Sc^{46}.

Thorium

The activity measured is from Pa^{233}. It is possible to resolve the absorption curve into two components, 0.05 and 0.30 Mev.

Barytes Concrete

The measured activity listed in Table V for Ba^{130} was determined using the analytical value of barium in the concrete. The approximately 60 day component

agrees with the analytical value of iron and the amount of 45 day activity induced in iron alloys. The 250 day activity corresponds to the analytical percentage of zinc using the cross section determined from the activity induced in the Zn in 72S aluminum.

Other Concretes and Graphite

The 15 hour component is Na^{24}. The 35 hour and the 85-100 day components may be composed of mixtures of isotopes as was found for beryllium. The 5.3y component is probably due to a trace of cobalt.

EXPERIMENTAL

Activity was measured with a high pressure ionization chamber which was calibrated with Co^{60} (which gives photons of 1.25 Mev average energy). Ionization chamber response is calculated for disintegrations of other isotopes relative to a value of 2.0 for a disintegration of Co^{60} (which gives 2 photons per disintegration), and are tabulated in Table IV. The response versus energy curve given in (1) was used to determine the response of photons of various energies.

Irradiations were conducted in the isotope stringer of the X-reactor where irradiation positions are calibrated in terms of the percentage of maximum thermal neutron flux. To obtain the average flux over the exposure period, the exposure expressed as kilowatt hours is divided by the exposure time in hours and multiplied by the percentage of maximum flux and by the maximum flux of 2.8×10^8 thermal neutrons/(sq cm, sec, kilowatt) given in (2). To put all the measurements on the basis of 10^{12} flux, values of induced activity are divided by the average value of thermal flux expressed as a fraction of 10^{12}.

In order that the measurements would not be affected by self-absorption, thin filings of the materials were irradiated. Check irradiations indicated reproducibility within about 5%. Activity measurements were not started until the sample had decayed from three to six hours; therefore, activities with half lives of less than an hour did not show up in most instances. Measurements for most of the materials were continued for more than a year.

BIBLIOGRAPHY

(1) J. W. Jones and R. T. Overman, The Use and Calibration of a 100% Geometry Ion Chamber, MonC-399 (1948), AECD-2367.

(2) J. W. Jones et al, Activation Measurement of the C-Neutron Flux in the Clinton Reactor, MonC-398 (1948).

(3) C. D. Bopp and O. Sisman, The Neutron Flux Spectrum and Fast and Epithermal Flux in Hole 19 of the ORNL Reactor, ORNL-525 (1950)

(4) National Bureau of Standards Circular 499, Nuclear Data (1950)

ACKNOWLEDGEMENTS

Where chemical analysis is shown rather than nominal composition, this analysis was made by the Analytical Chemistry Division.

APPENDIX I

Calculation of Roentgens Equivalent Physical per Hour

Since the principal use for induced activity data will be in shielding calculations, and for personnel protection, it will generally be necessary to convert the preceding data from gamma flux to roentgens per hour.

The gamma flux in photons/(sec, sq cm) is related to the roentgens equivalent physical/hour by the absorption coefficient of tissue for the gamma radiation, the energy of the radiation, and an energy conversion factor:

$$\text{rep/hr} = (N/A)\ E\ K\ \mu_m \qquad \text{equation 5}$$

where (N/A) = the number of photons/second crossing unit area, photons/(sec, sq cm)

E = the energy of the photons, Mev

μ_m = the mass absorption coefficient for the photons in tissue = about 0.03 sq cm/gm for photon energies from about 0.5 to 2 Mev

K = a conversion factor = 1.6×10^{-6} ergs/Mev x 1 rep gm/83 ergs x 3600 sec/hr = 7×10^{-5} rep, gm, sec/(Mev, hr)

Example: Calculate the rep at a distance of 1.0 cm from a 10^6 photon/sec point source of 1.0 Mev photons. The area over which the photons are distributed is:

$A = 4\pi r^2 = 4 \times 3.14 \times (1.0)^2 = 12.56$ sq cm. Substituting in eq 5 gives rep/hr =

$(10^6/12.56) \times 1.0 \times 0.03 \times 7 \times 10^{-5} = 0.135$ rep/hr

APPENDIX II

Decay Curves

UNCLASSIFIED
SSD-A-644
DWG. 17557

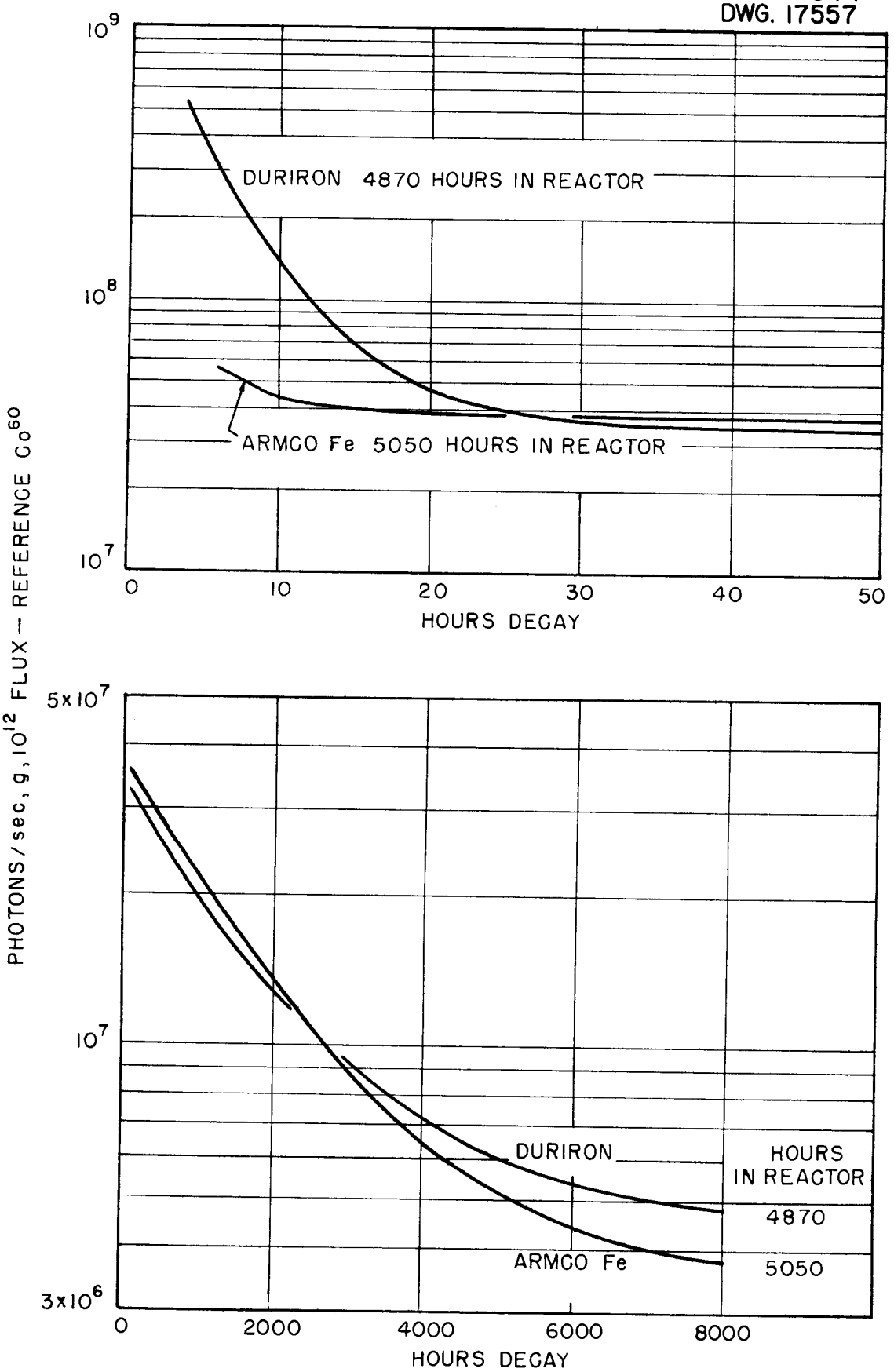

Fig. A1 — Gamma Decay of Armco Iron and Duriron

UNCLASSIFIED
SSD-A-645
DWG. 17558

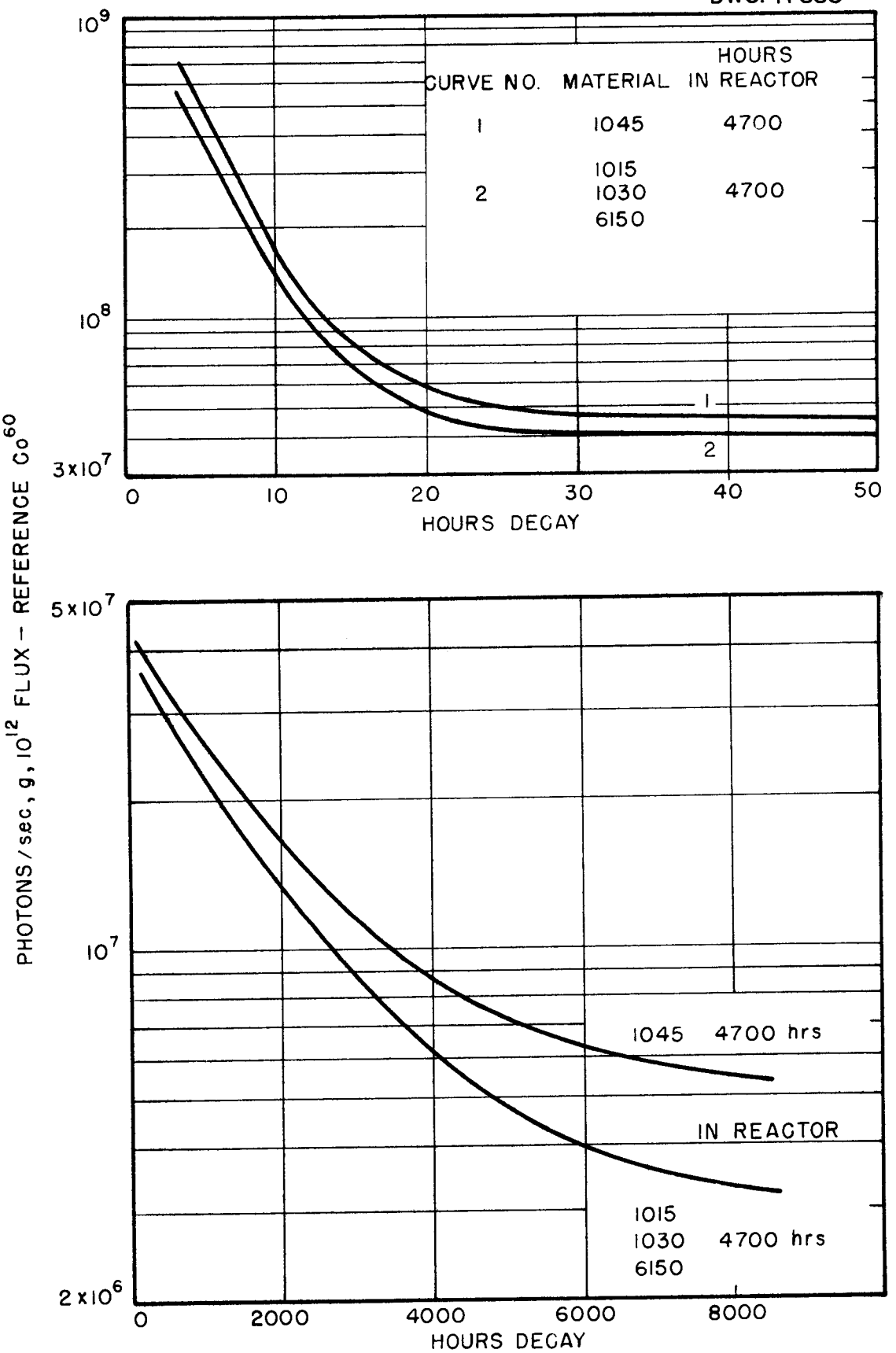

Fig. A 2 - Gamma Decay of 1015, 1030, 1045 and 6150 Iron Alloys

UNCLASSIFIED
SSD-A-646
DWG. 17559

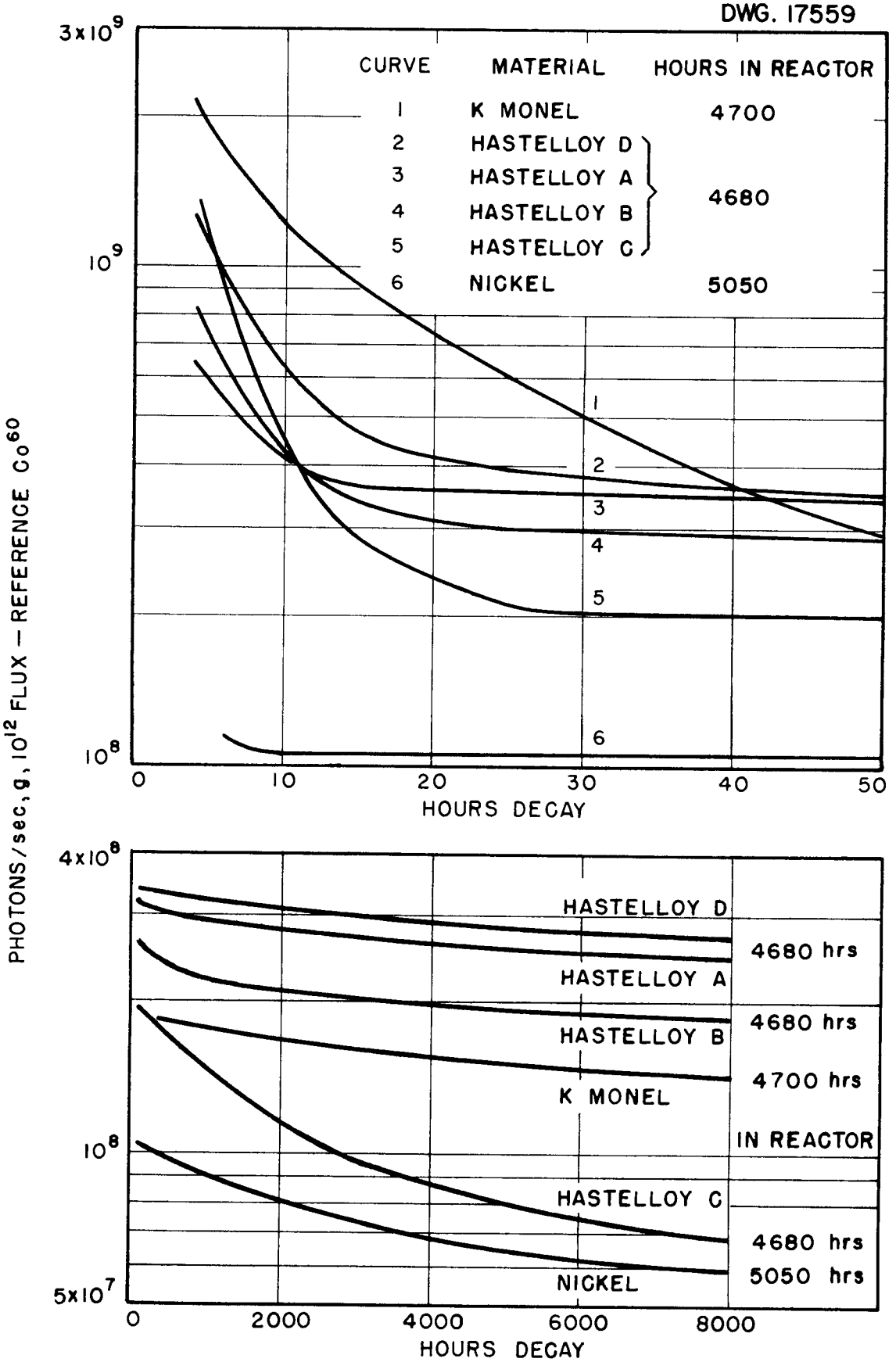

Fig. A 3 Gamma Decay of Nickel, K Monel and Hastelloys

UNCLASSIFIED
SSD-A-647
DWG. 17560

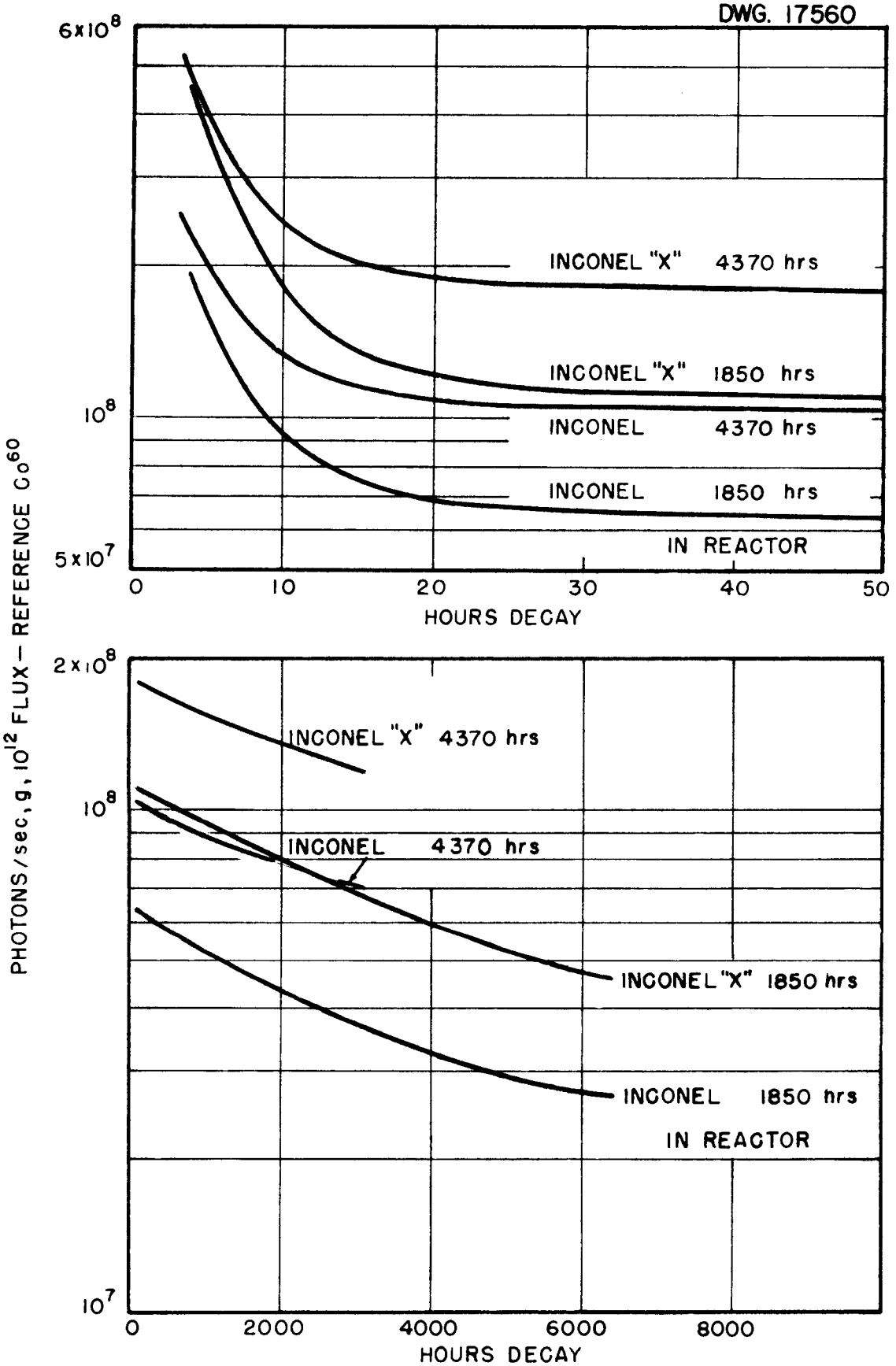

Fig. A 4 Gamma Decay of Inconel and Inconel X

UNCLASSIFIED
SSD-A-648
DWG. 17561

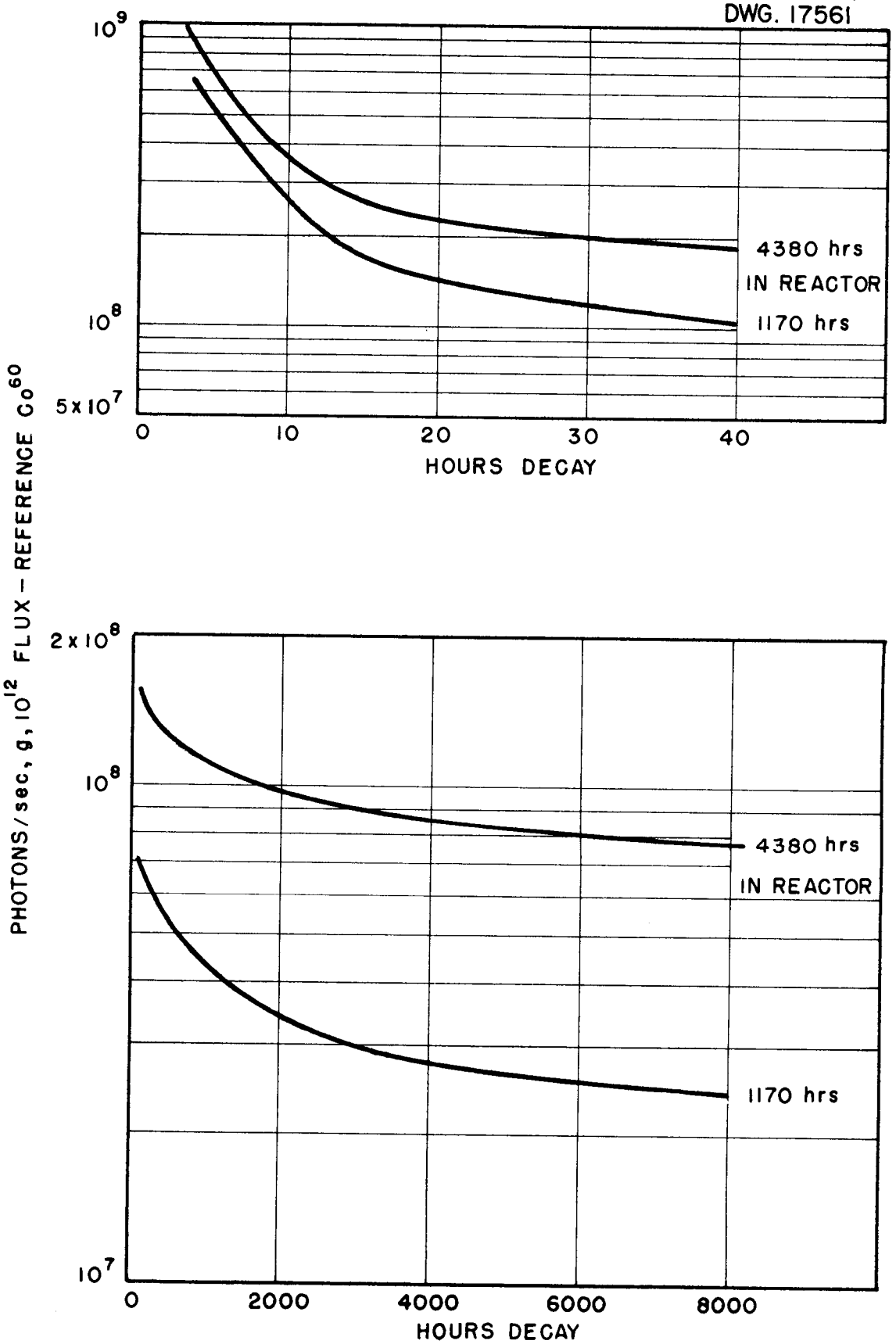

Fig. A5 Gamma Decay of Carpenter 20 Steel

UNCLASSIFIED
SSD-A-649
DWG. 17562

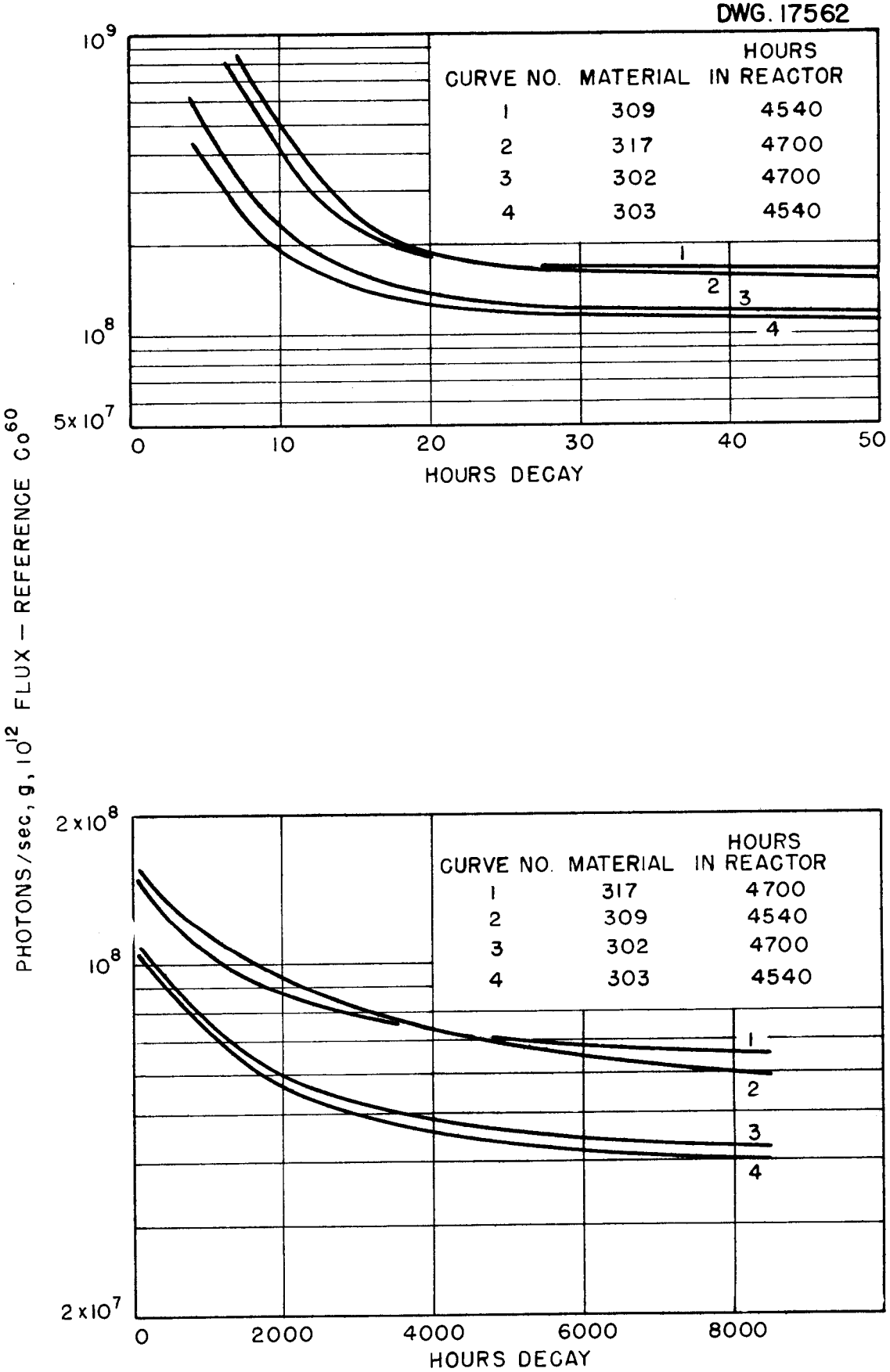

Fig. A6 Gamma Decay of 302, 303, 309, and 317 Steels

UNCLASSIFIED
SSD-A-650
DWG. 17563

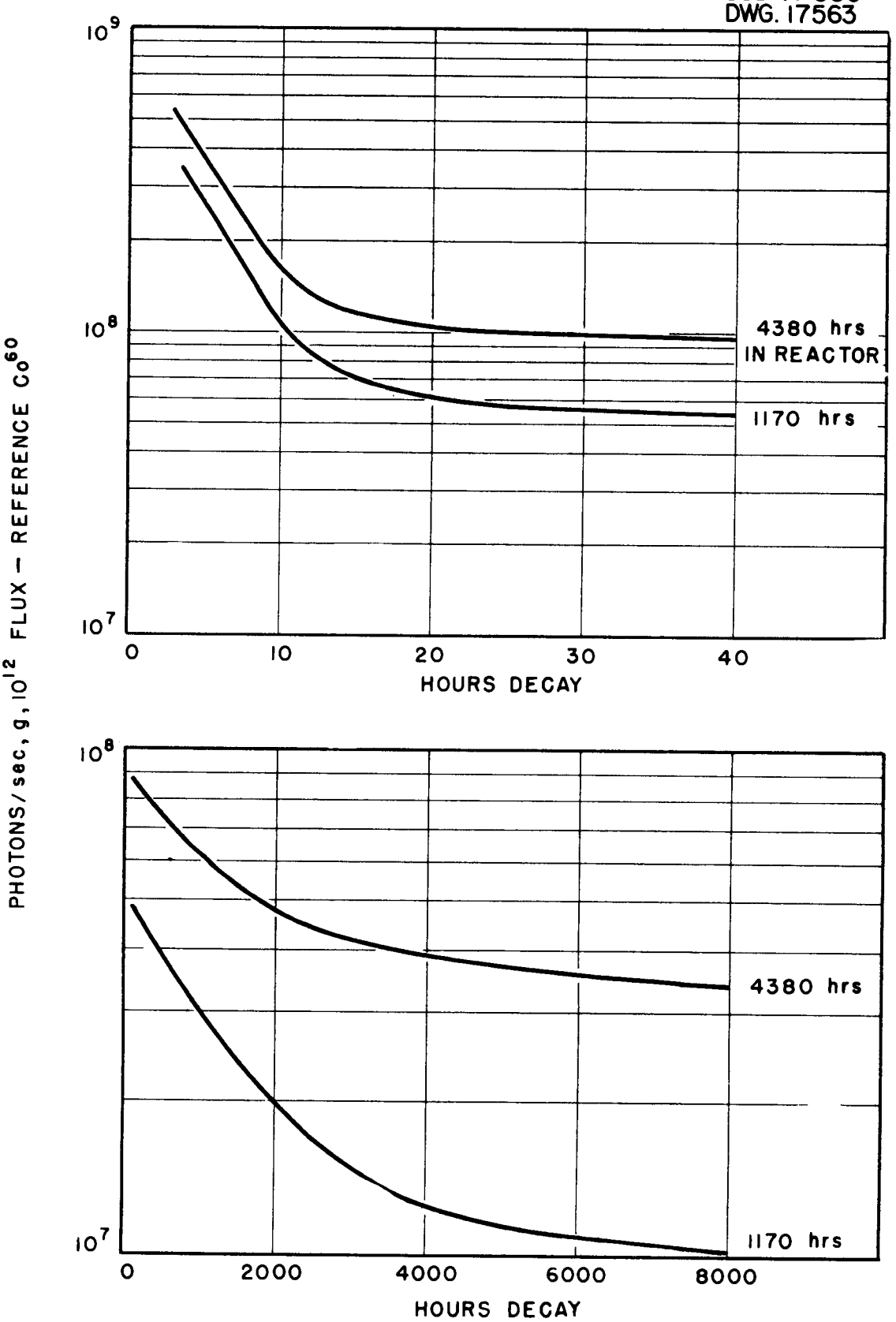

Fig. A7 Gamma Decay of 304 Steel

UNCLASSIFIED
SSD-A-651
DWG. 17564

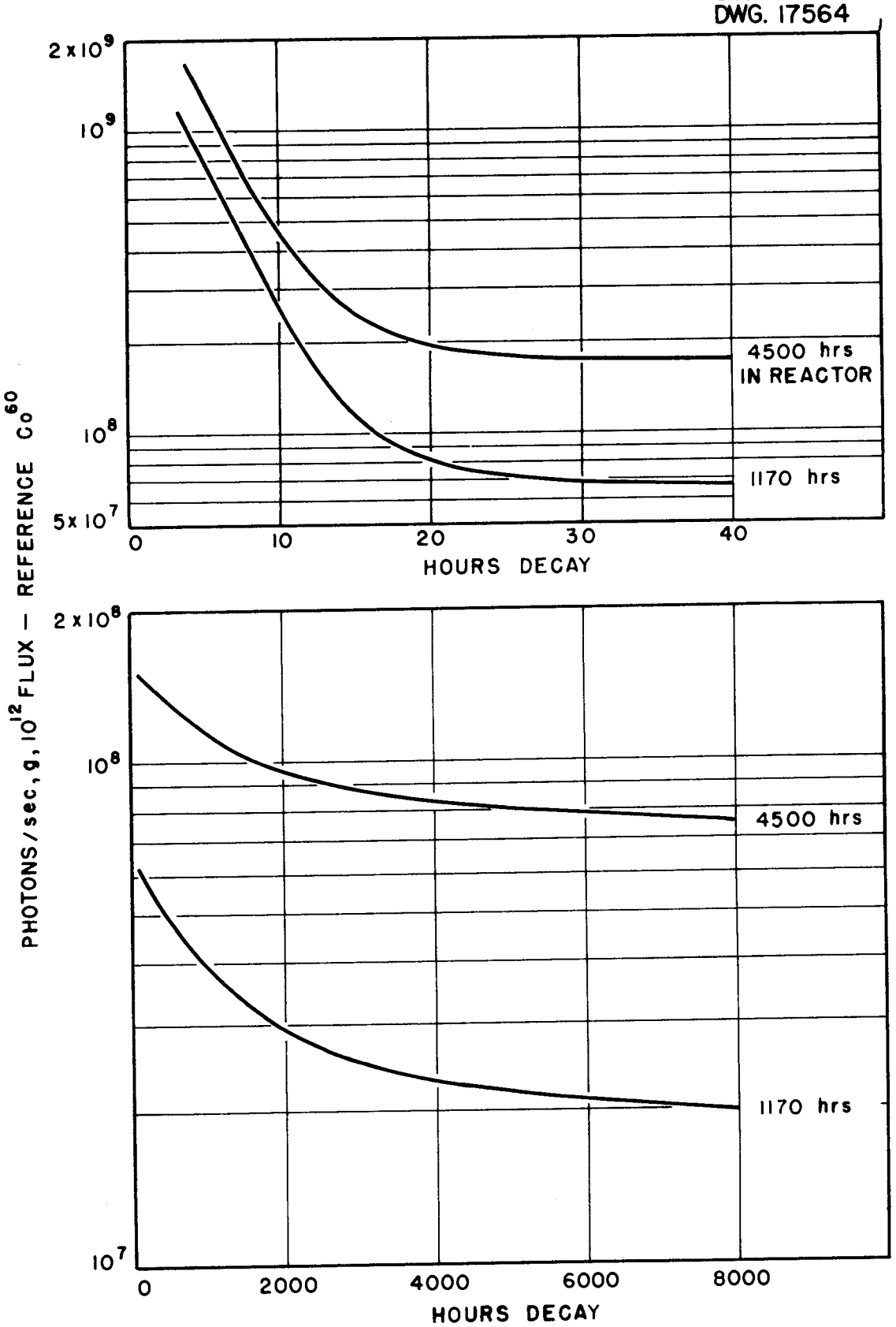

Fig. A8 Gamma Decay of 310 Steel

UNCLASSIFIED
SSD-A-652
DWG. 17565

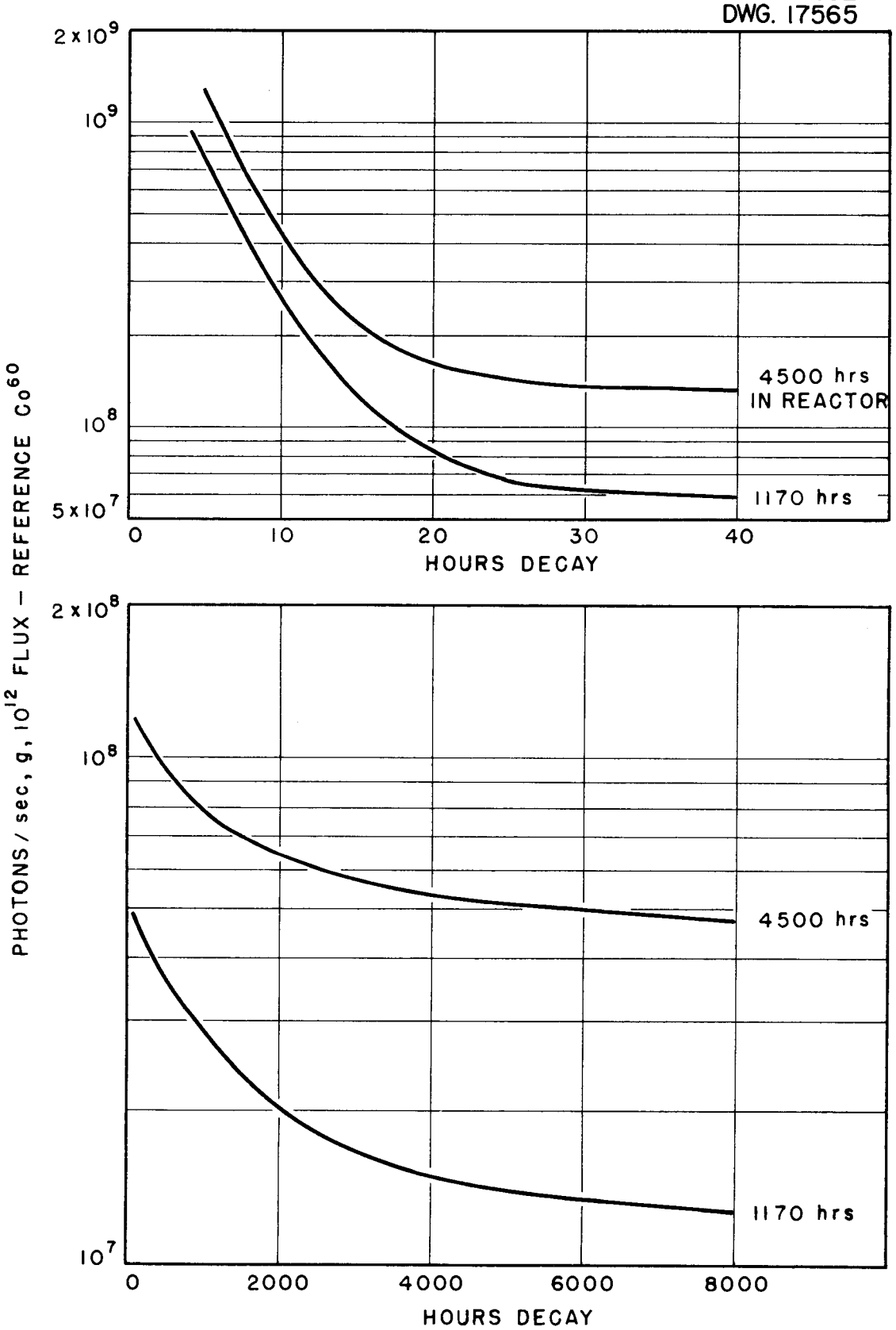

Fig. A9 Gamma Decay of 316 Steel

UNCLASSIFIED
SSD-A-653
DWG. 17566

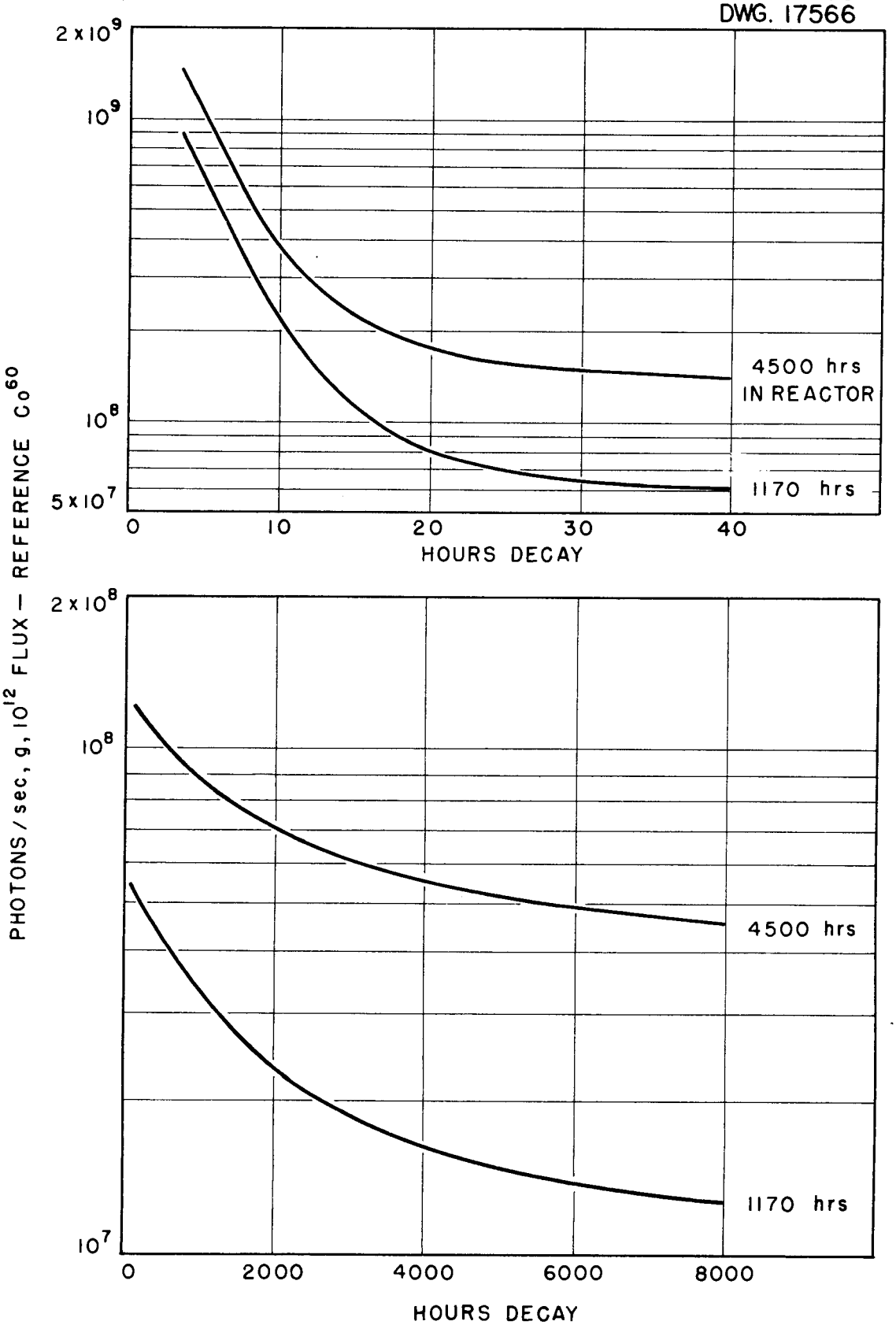

Fig. A10 Gamma Decay of 347 Steel

UNCLASSIFIED
SSD-A-654
DWG. 17567

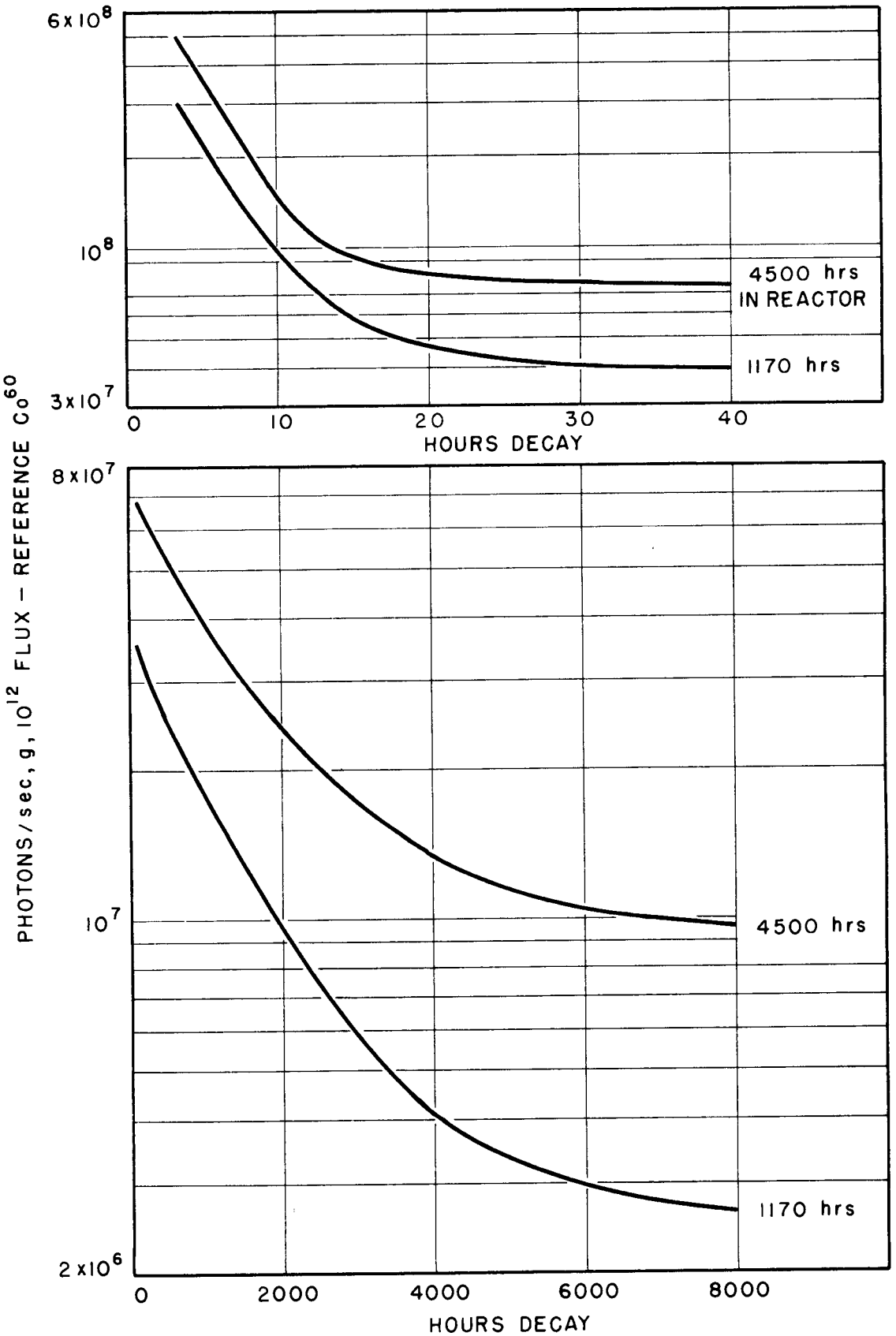

Fig. A11 Gamma Decay of 405 Steel

UNCLASSIFIED
SSD-A-655
DWG. 17568

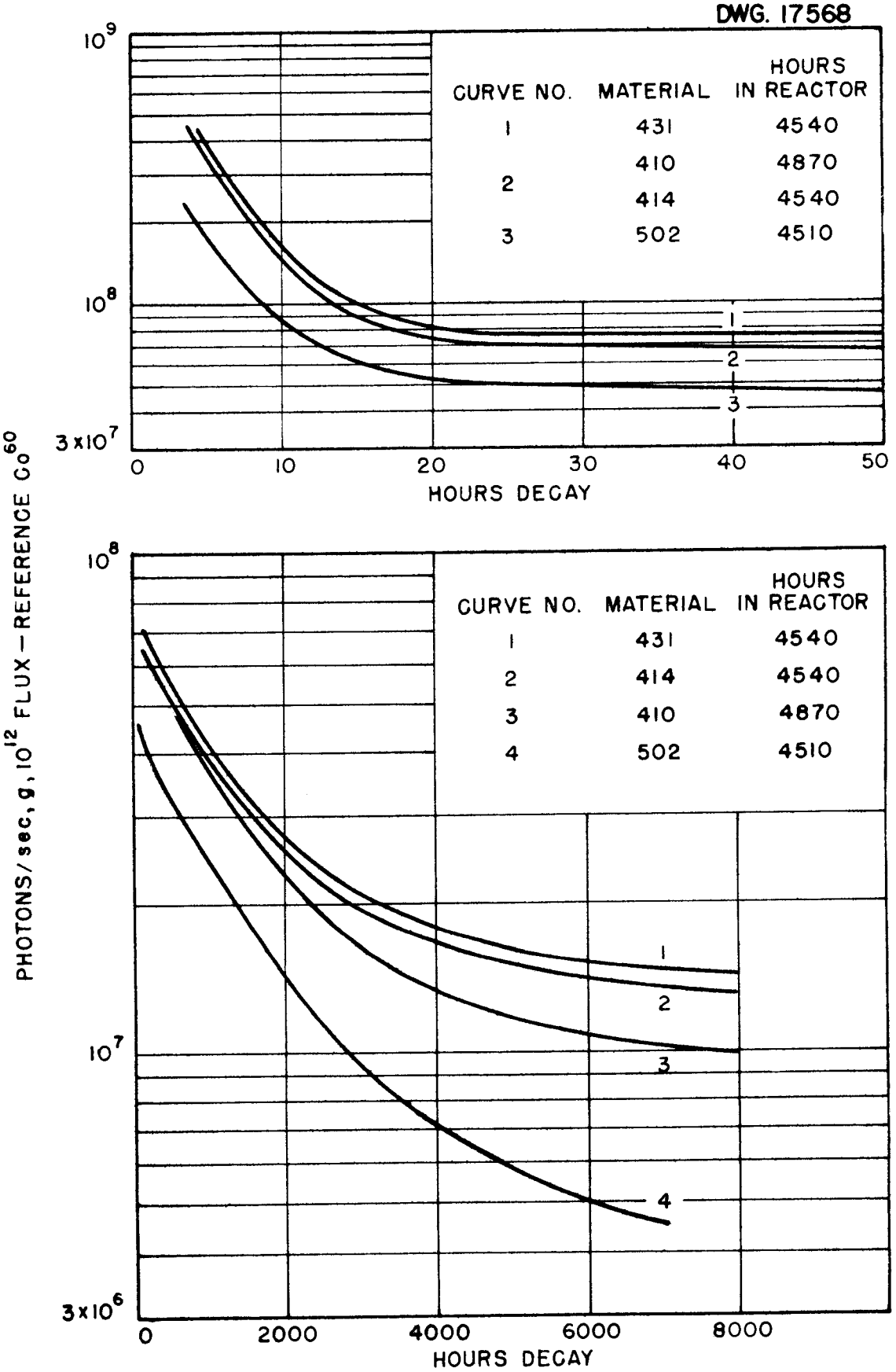

Fig. A12 Gamma Decay of 410, 414, 431, 502 Steels

UNCLASSIFIED
SSD-A-656
DWG. 17569

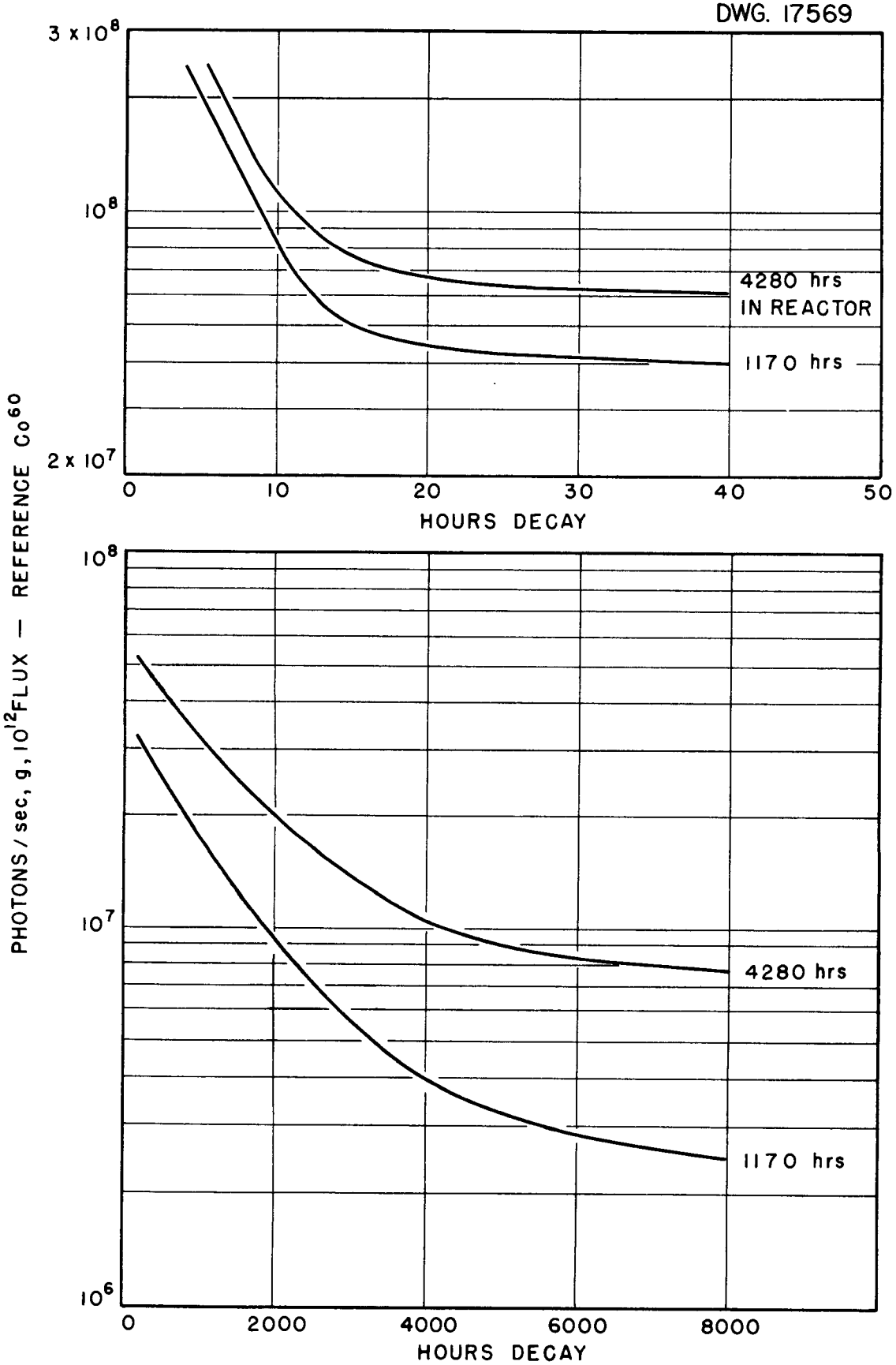

Fig. A13 Gamma Decay of 430 Steel

UNCLASSIFIED
SSD-A-657
DWG. 17570

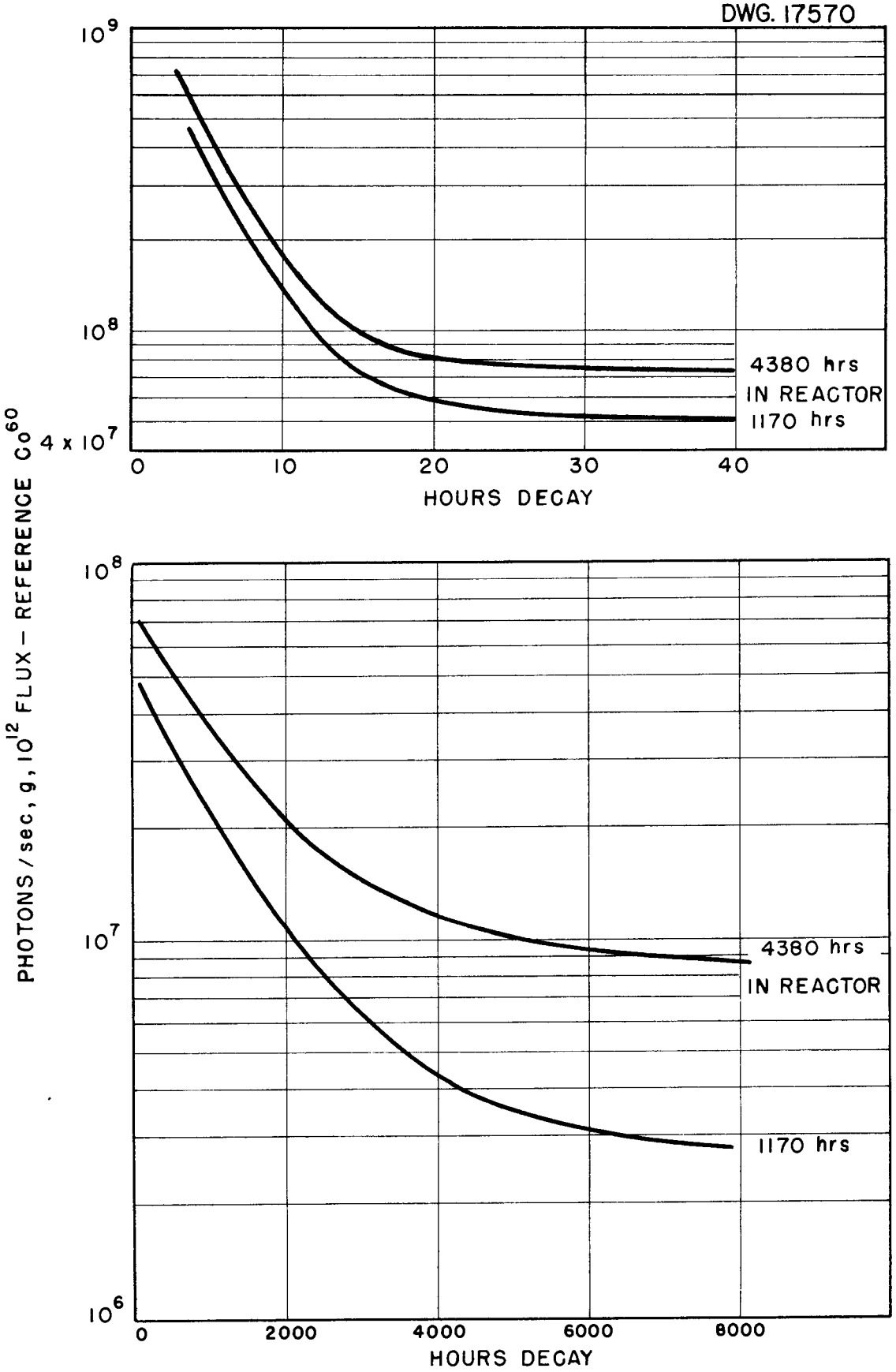

Fig. A14 Gamma Decay of 446 Steel

UNCLASSIFIED
SSD-A-658
DWG. 17571

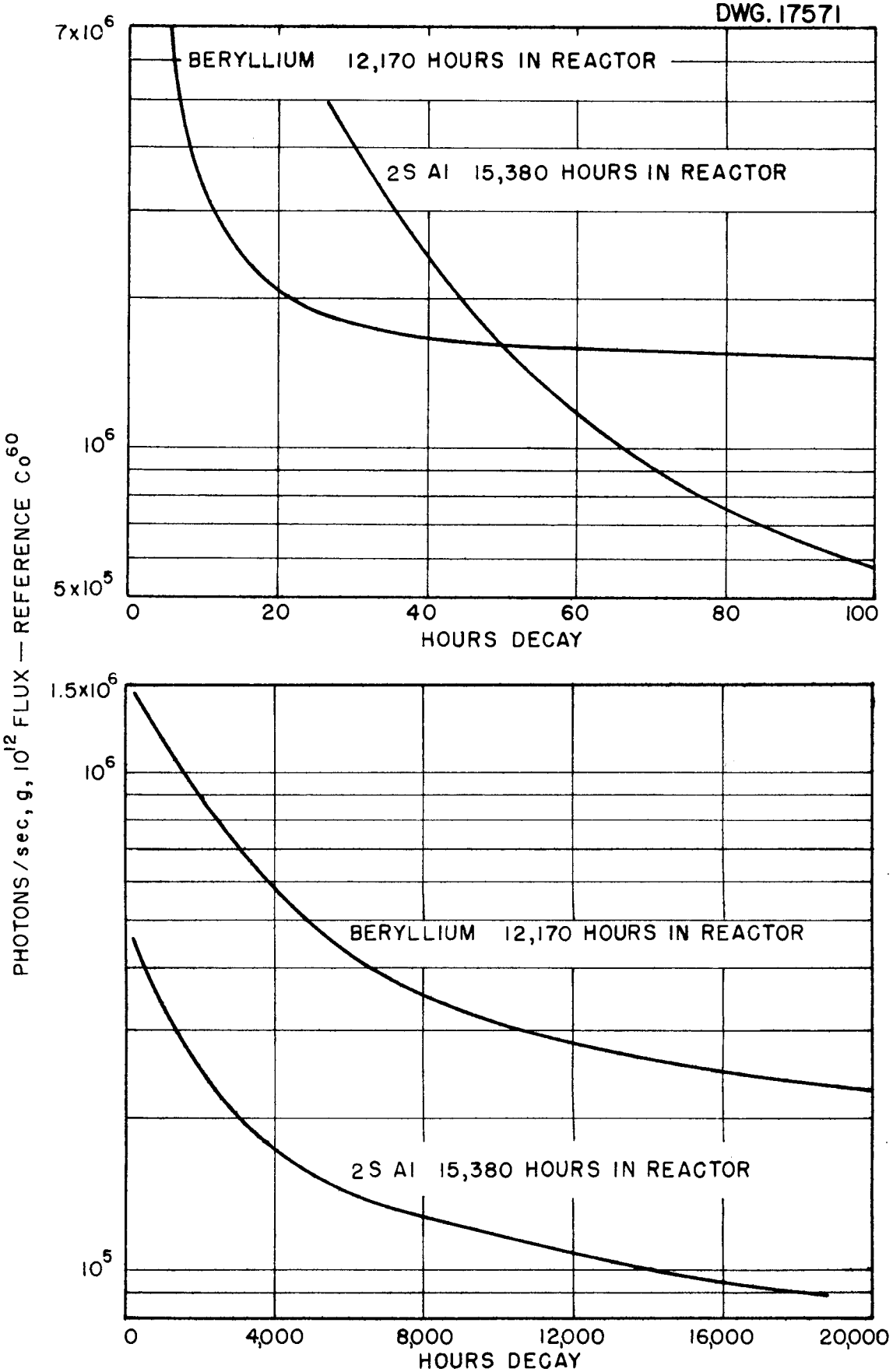

Fig. A15 Gamma Decay of 2S Aluminum and Beryllium

UNCLASSIFIED
SSD-A-659
DWG. 17572

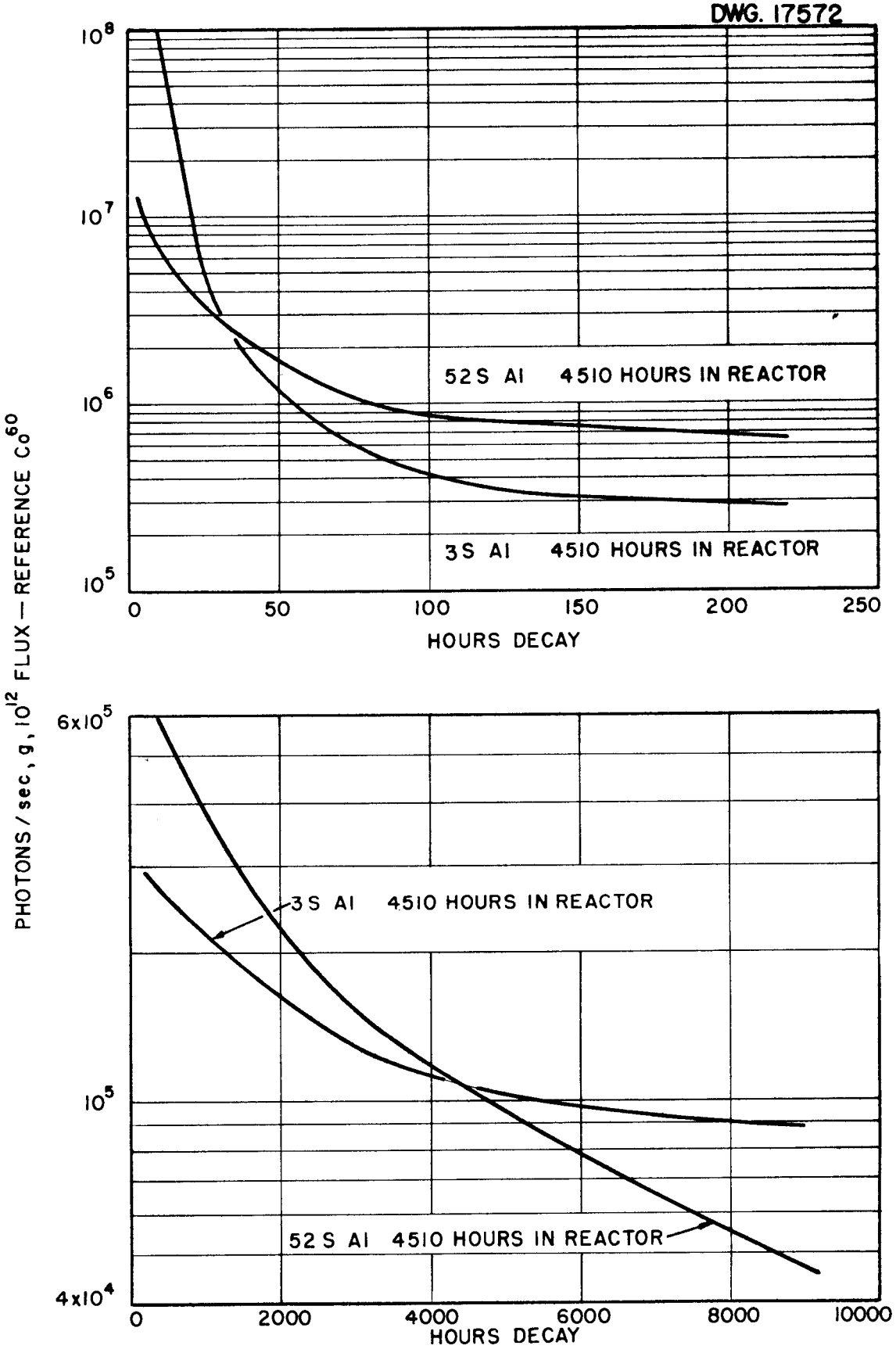

Fig. A16 Gamma Decay of 3S and 52S Aluminum

UNCLASSIFIED
SSD-A-660
DWG. 17573

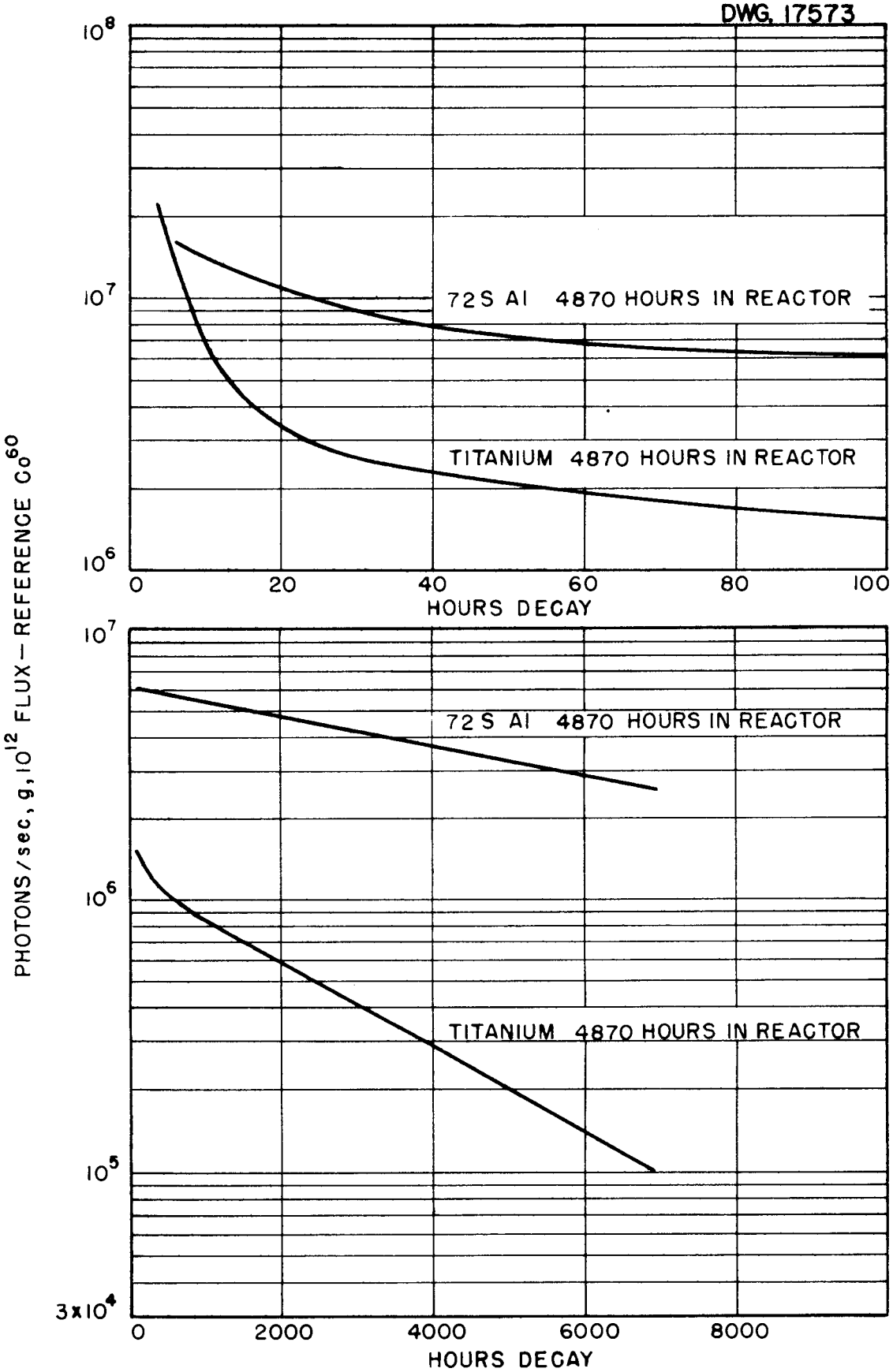

Fig. A17 Gamma Decay of 72 S Aluminum and Titanium

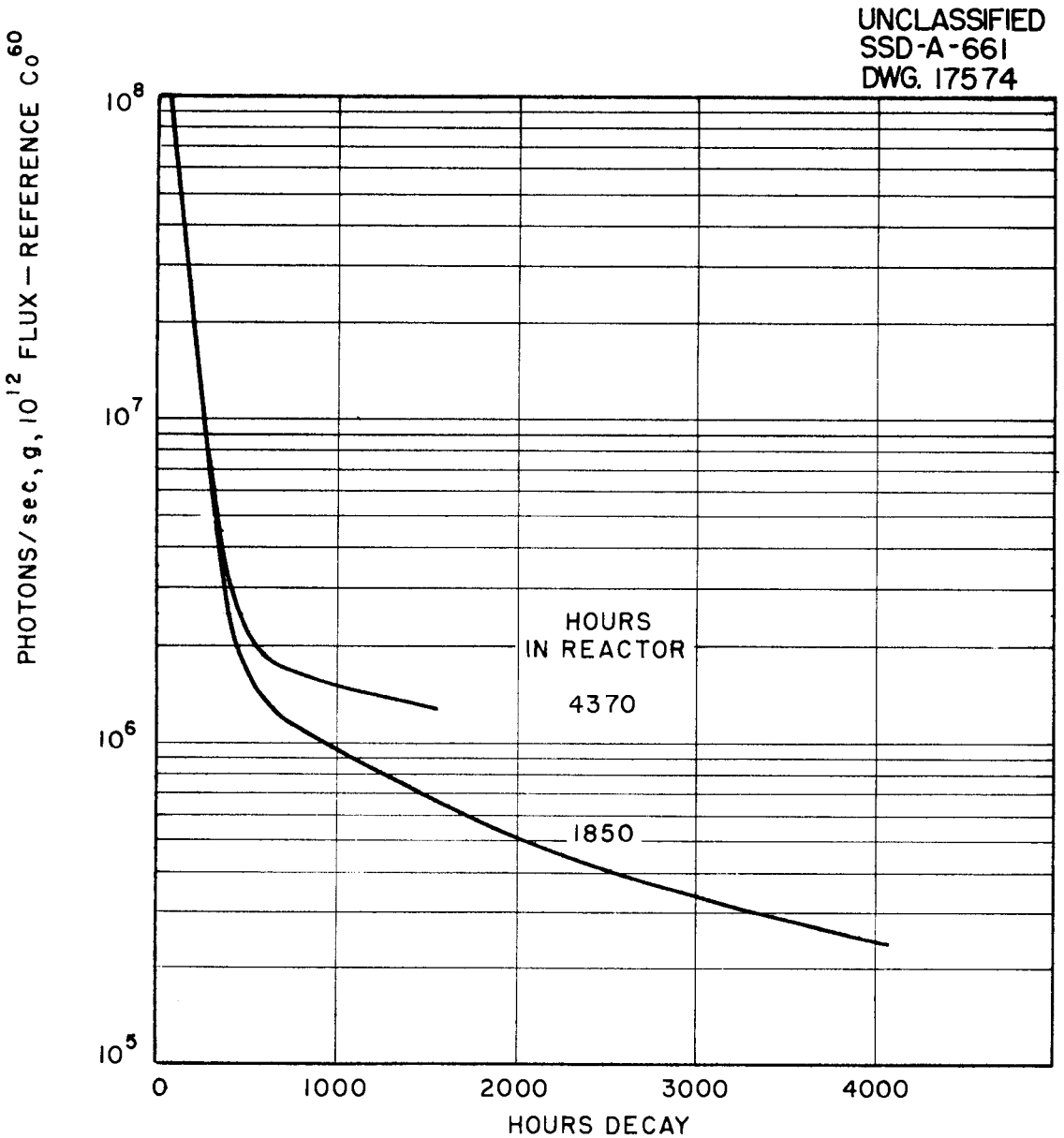

Fig. A18 Gamma Decay of Cadmium

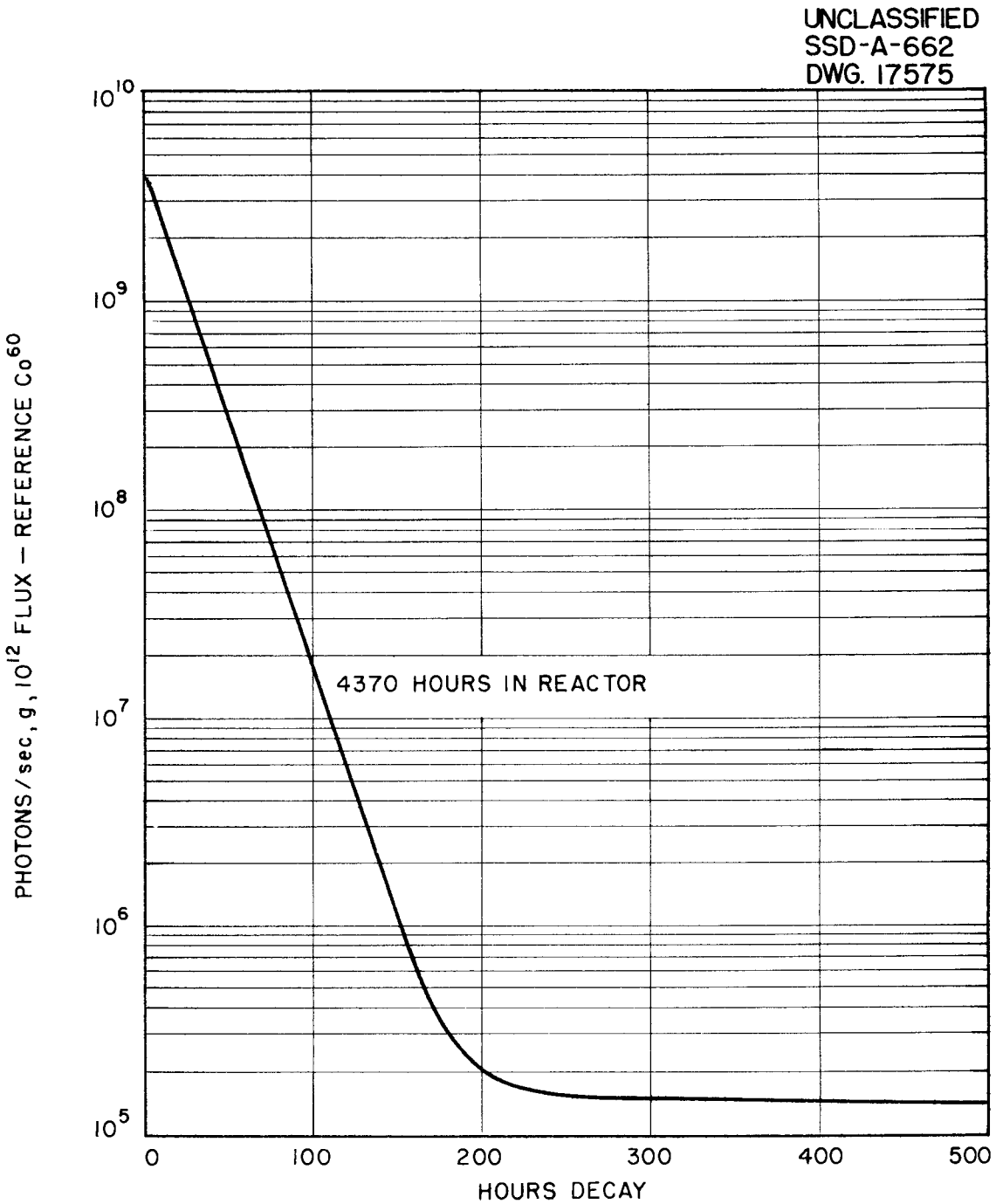

Fig. A19 Gamma Decay of Copper

UNCLASSIFIED
SSD-A-663
DWG. 17576

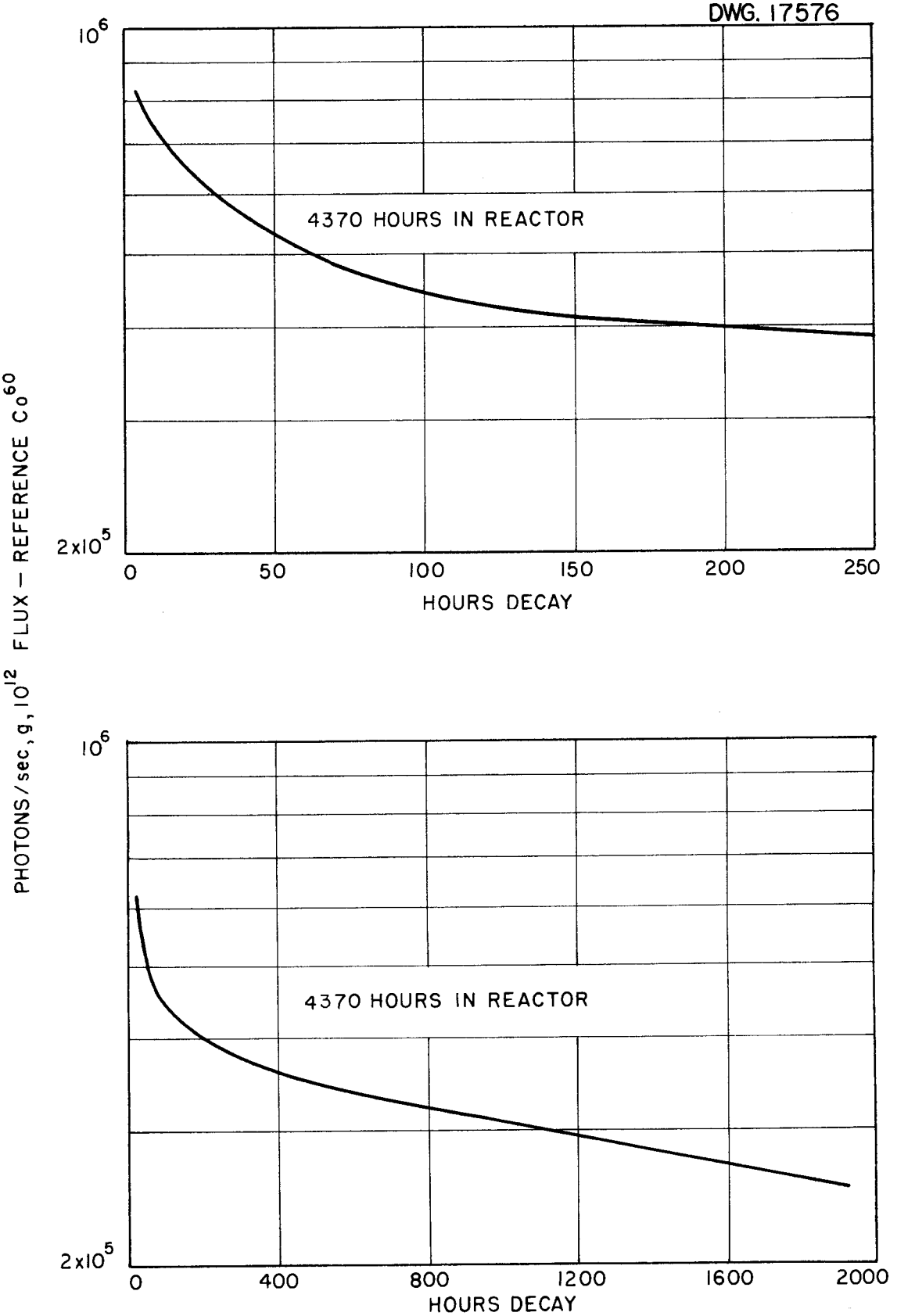

Fig. A20 Gamma Decay of Lead

UNCLASSIFIED
SSD-A-664
DWG. 17577

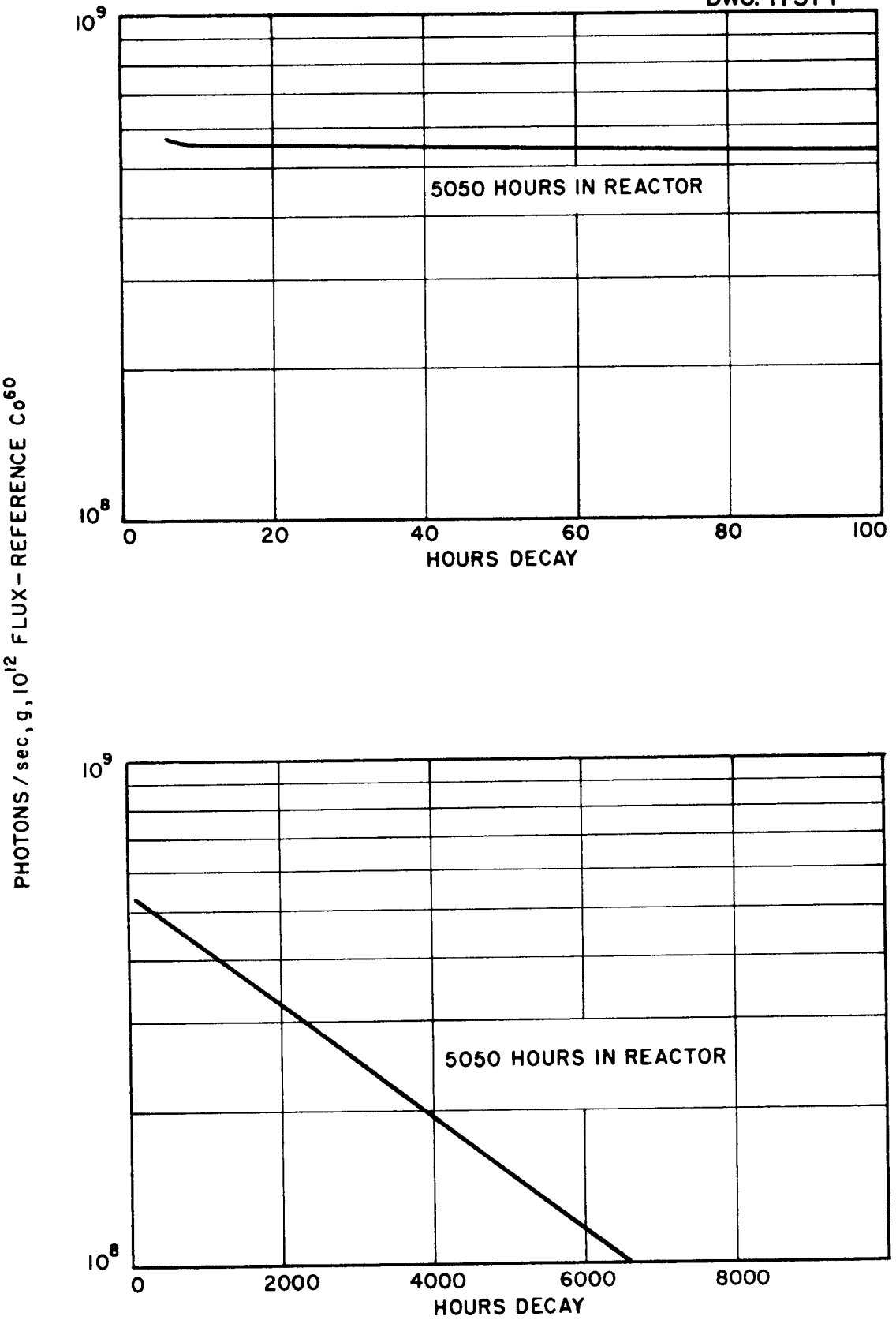

Fig. A 21 Gamma Decay of Niobium

[redacted]
SSD-A-665
DWG. 17578

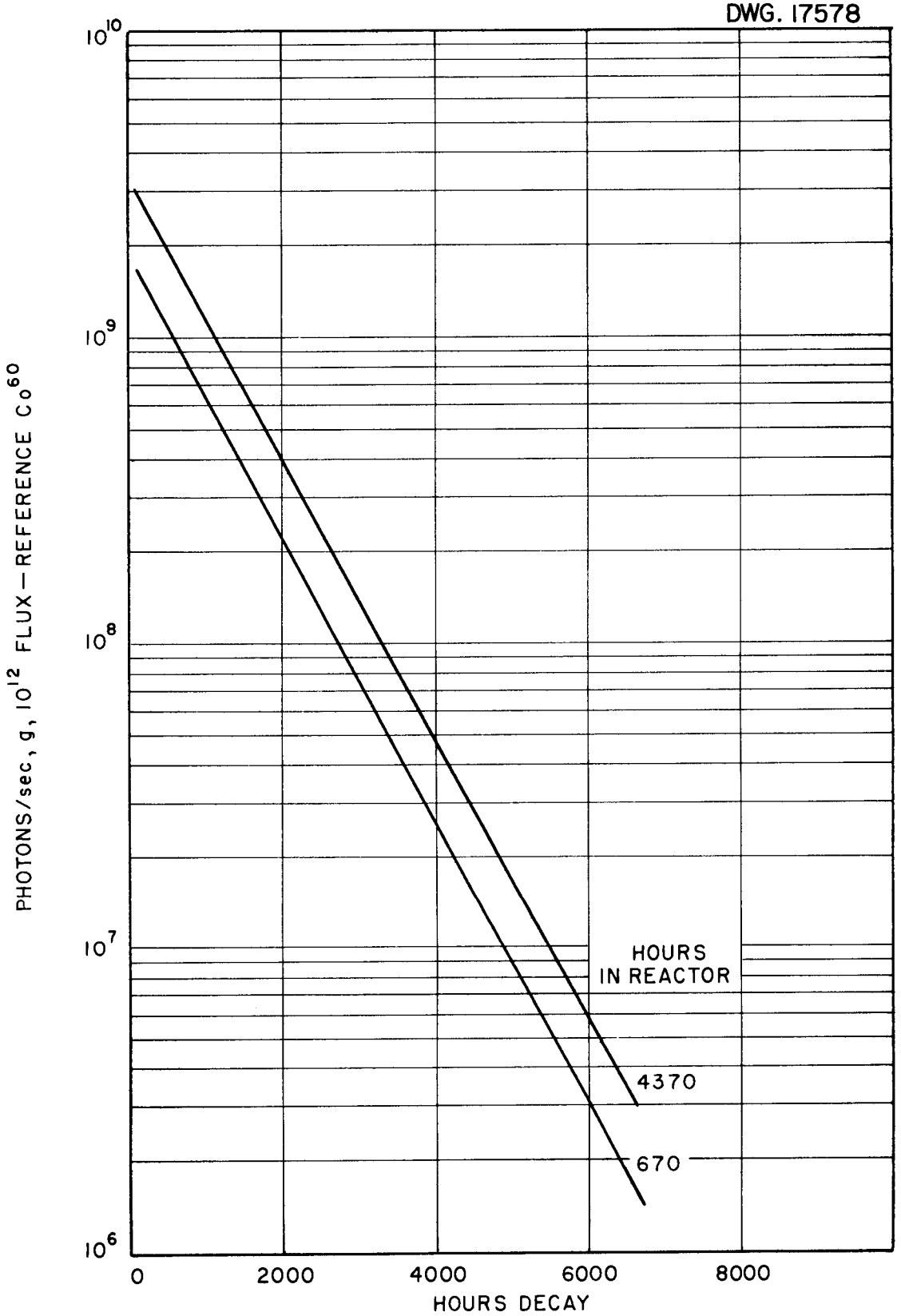

Fig. A 22 Gamma Decay of Thorium

UNCLASSIFIED
SSD-A-666
DWG. 17579

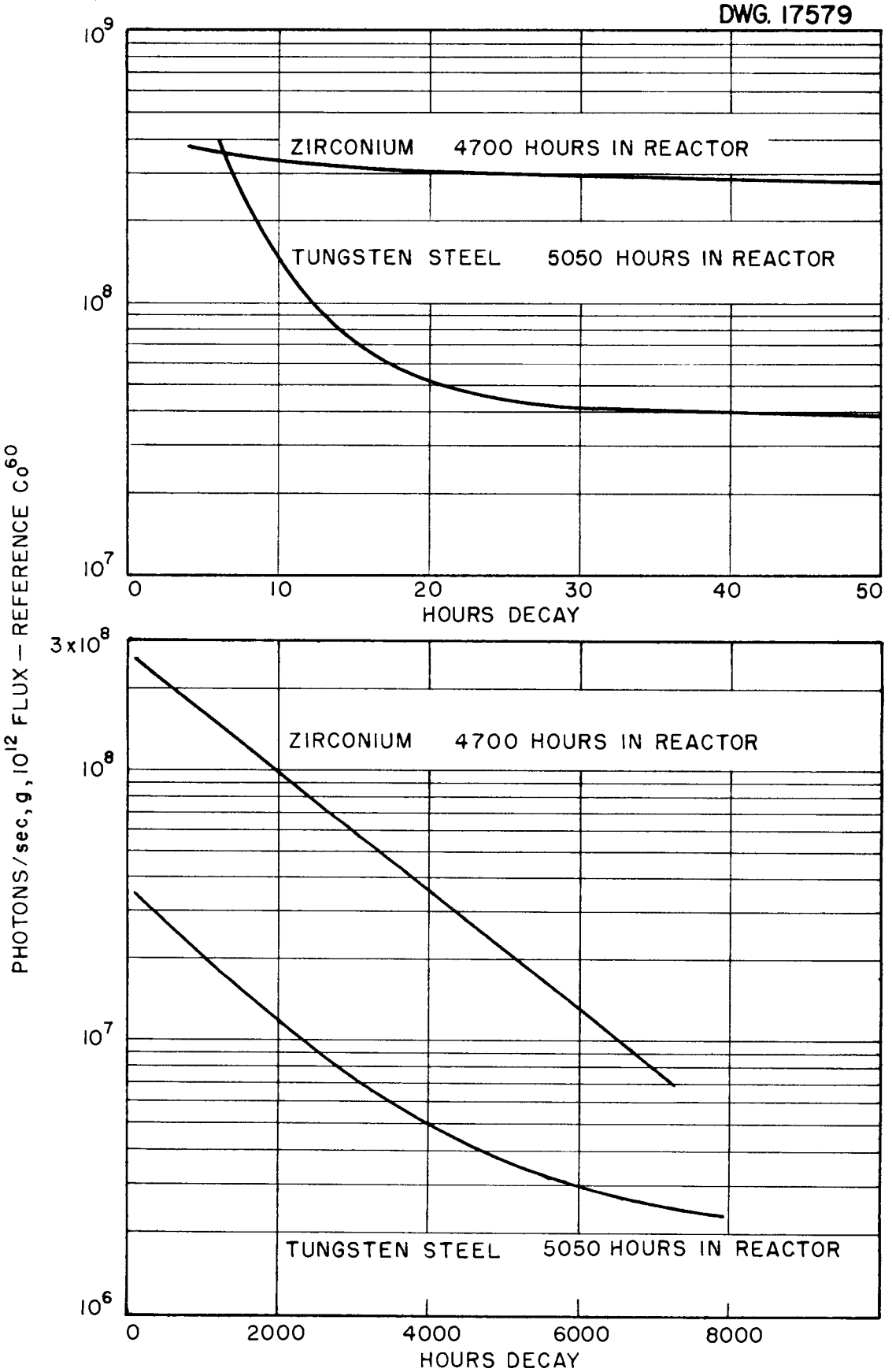

Fig. A23 Gamma Decay of Zirconium, Tungsten Steel

UNCLASSIFIED
SSD-A-667
DWG. 17580

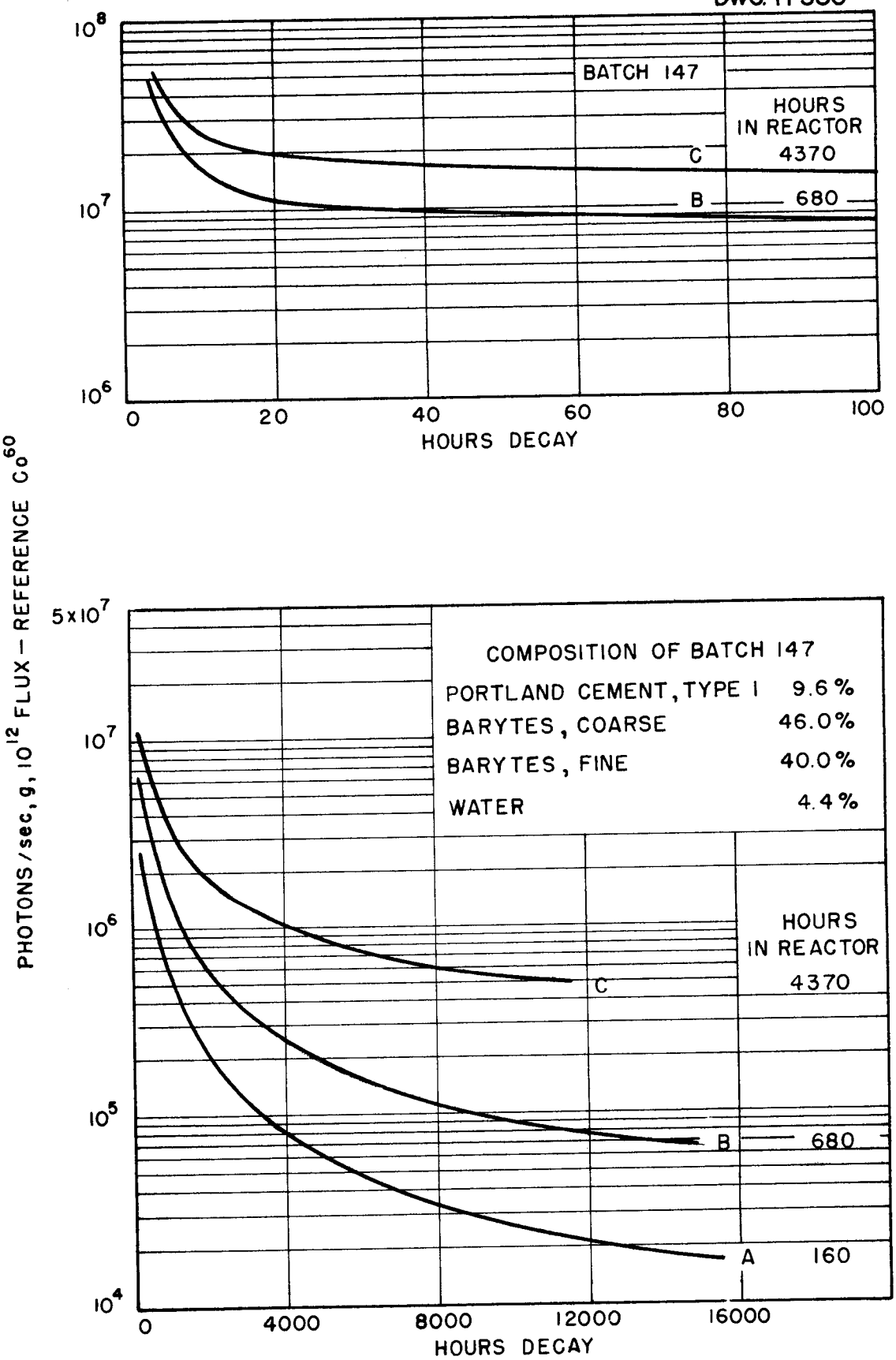

Fig. A24 Gamma Decay of Barytes Concrete

UNCLASSIFIED
SSD-A-668
DWG. 17581

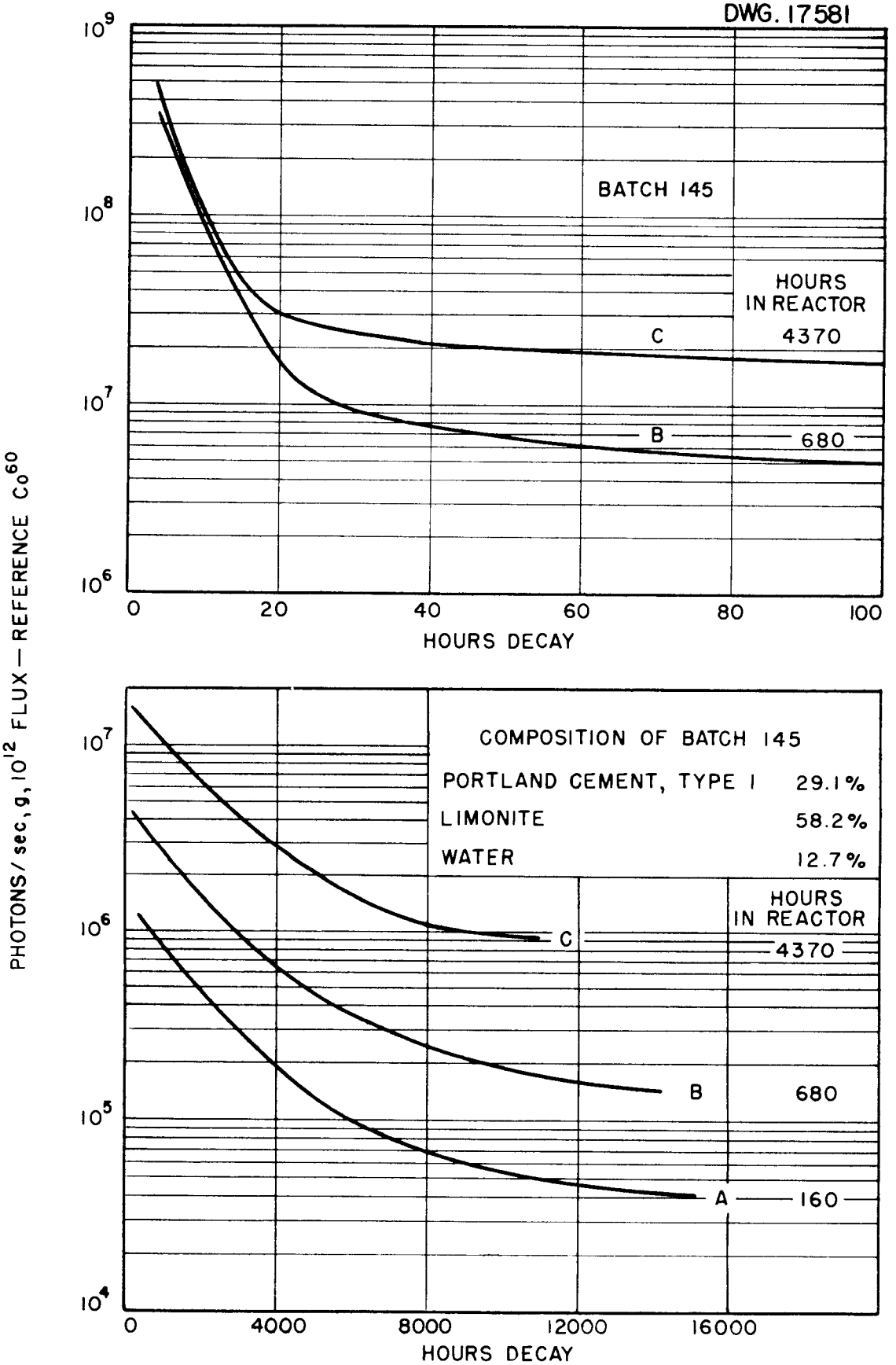

Fig. A25 Gamma Decay of Brookhaven Cement

UNCLASSIFIED
SSD-A-669
DWG. 17582

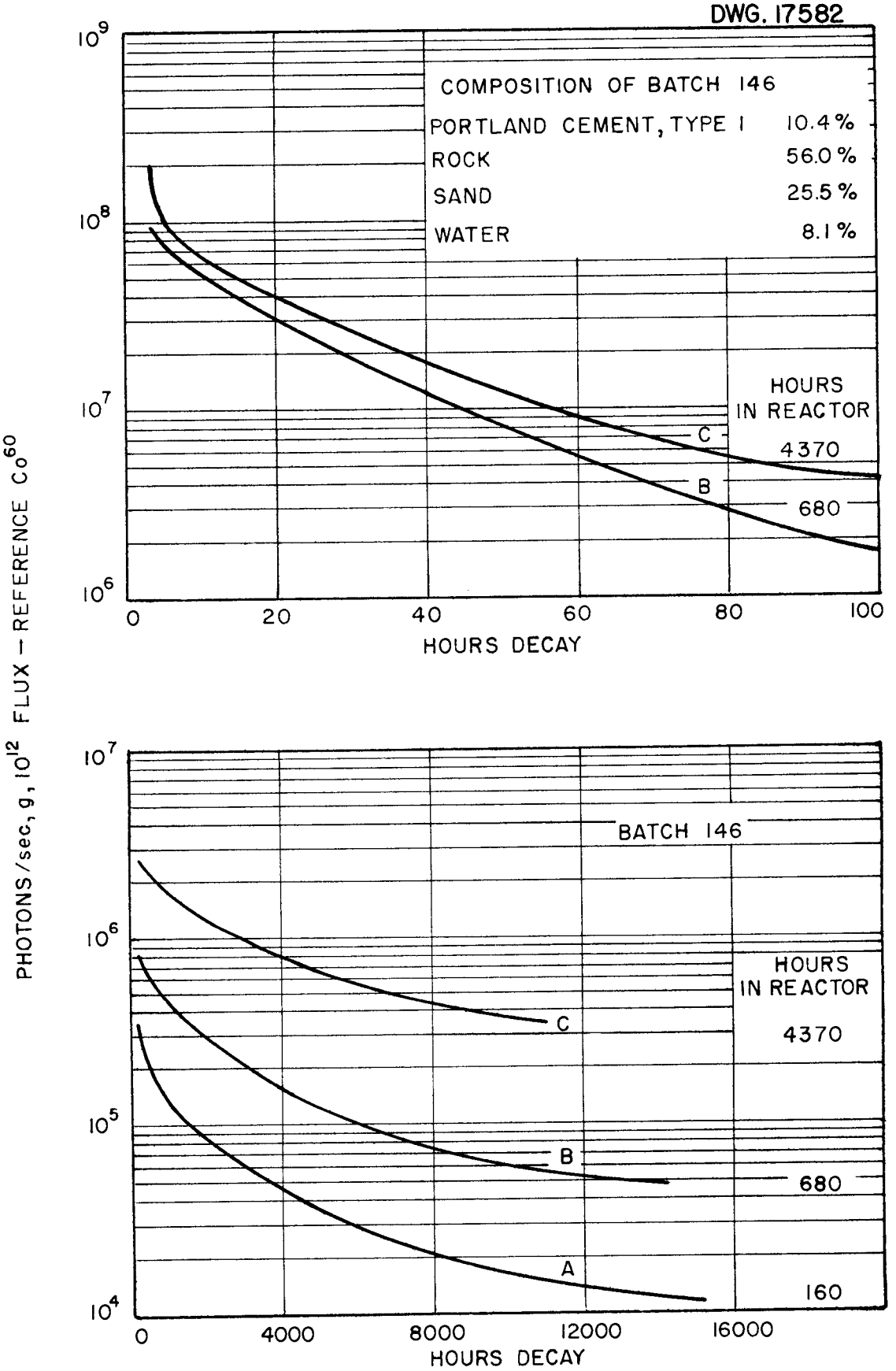

Fig. A26 Gamma Decay of Portland Concrete

[redacted]

SSD-A-670
DWG. 17583

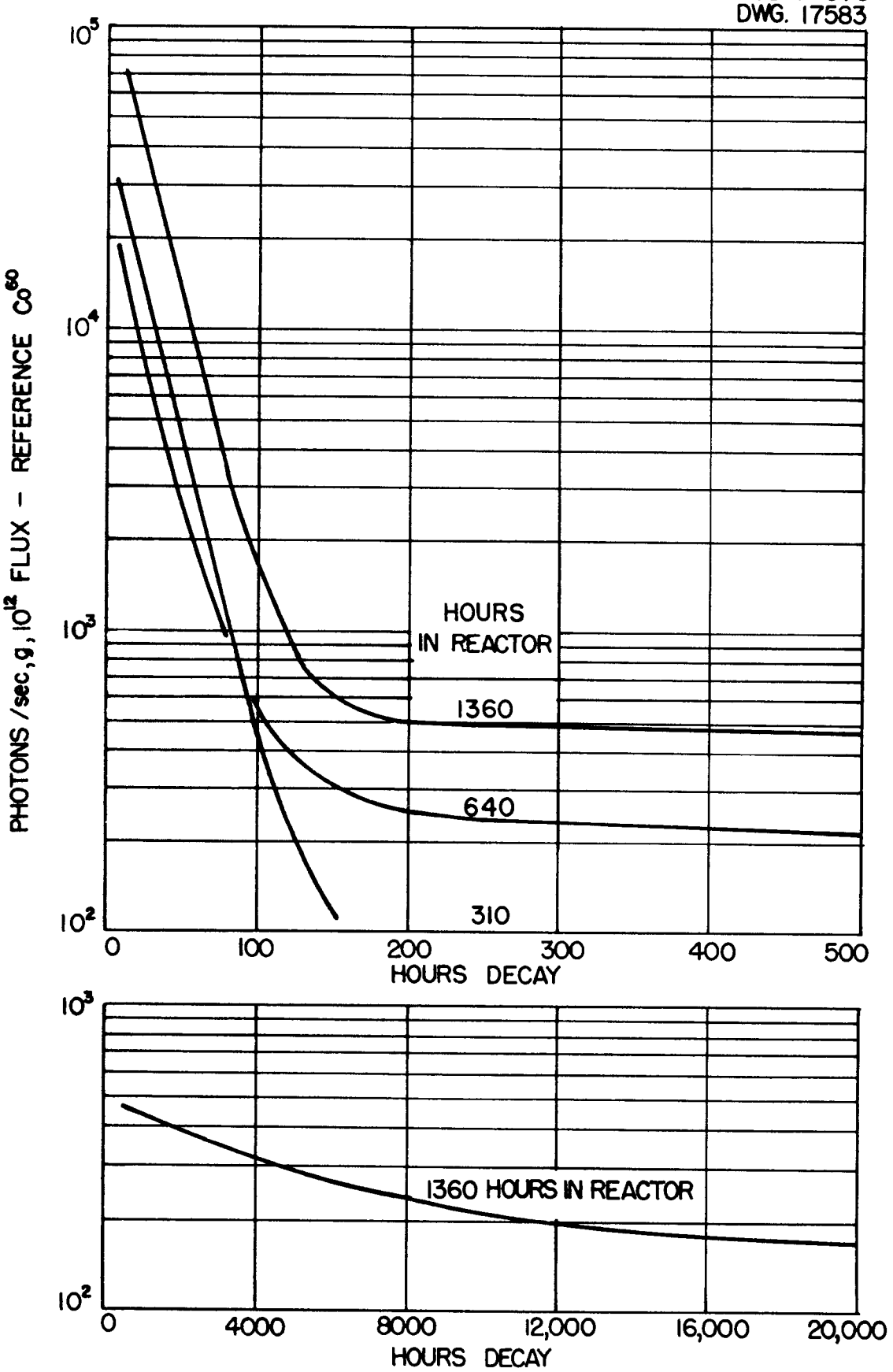

Fig. A27 Gamma Decay of GBF Graphite

[redacted]
SSD-A-671
DWG. 17584

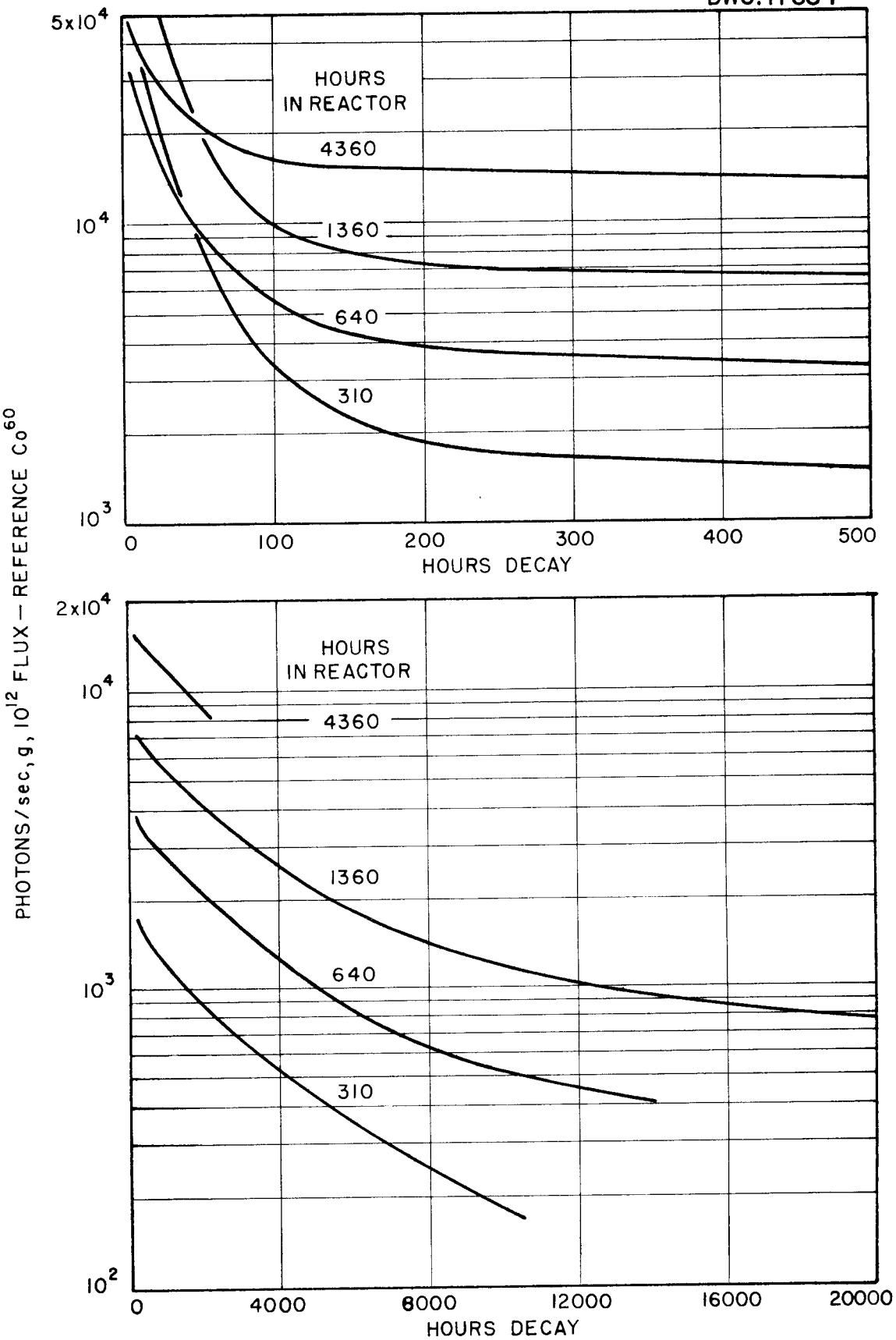

Fig. A 28 Gamma Decay of CS Graphite

[redacted]
SSD-A-672
DWG. 17585

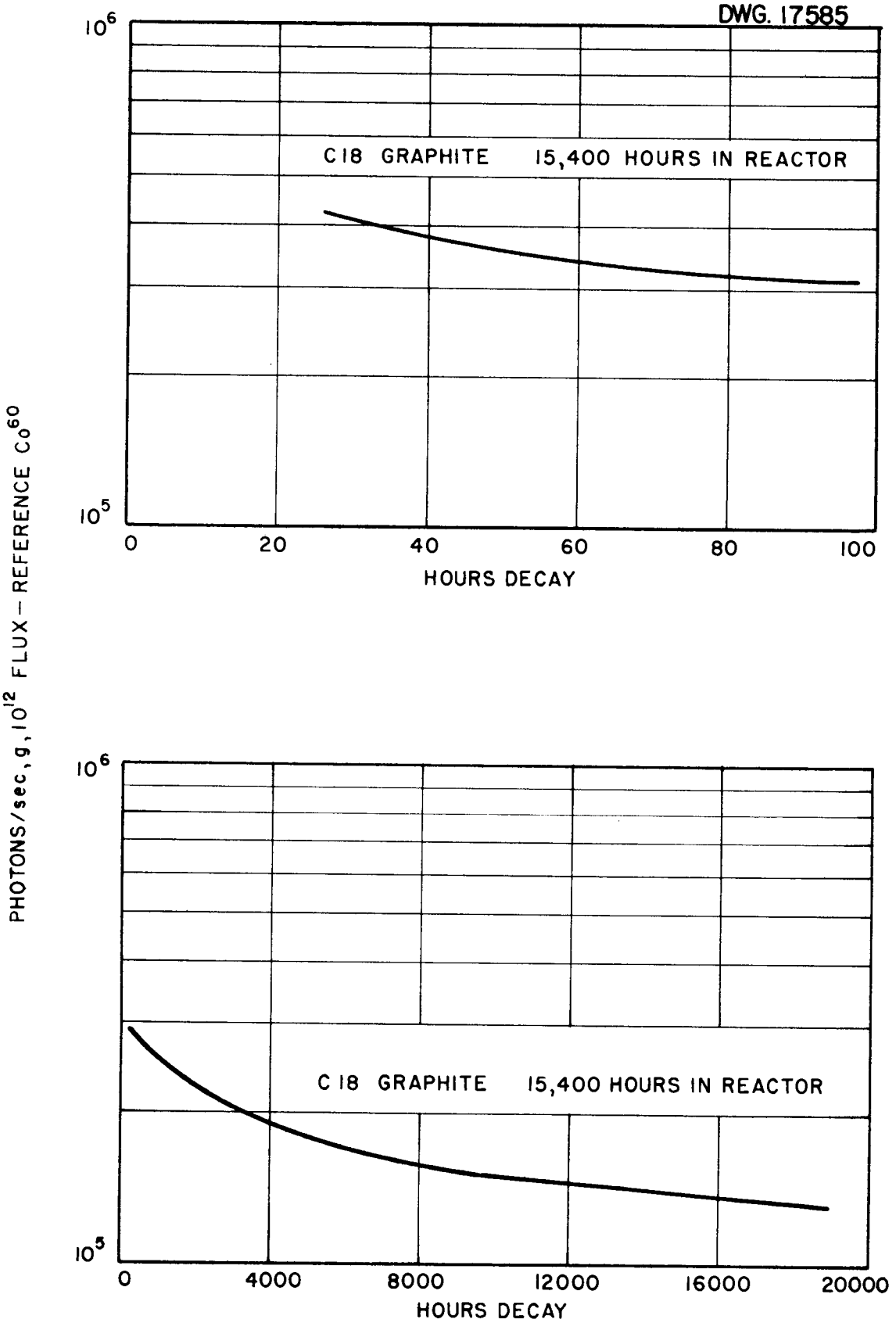

Fig. A 29 Gamma Decay of C18 Graphite